



Developing a 3D hydrostratigraphical model of the emerged part of the Pelotas Basin along the northern coast of Rio Grande do Sul state, Brazil

Luciano Marquetto^{1,6} · Alexander Jüstel^{2,3} · Guilherme Casarotto Troian⁴ · Pedro Antonio Roehe Reginato⁵ · Jefferson Cardia Simões⁶

Received: 31 October 2023 / Accepted: 18 April 2024

© The Author(s) 2024

Abstract

The coastal plain of Rio Grande do Sul state, in Brazil, is highly vulnerable to expected changes in sea level, while having an increasing population and consequently increasing water demands. Adequate management is essential to restrain contamination, depletion and salinization of the region's aquifers considering current and future challenges, but geologic knowledge is essential to guide groundwater sustainable practices. To contribute to this discussion, this work integrated existing geological data from the northern coast of Rio Grande do Sul state to create a three-dimensional representation of the main hydrostratigraphical units of the region and its relation to the basement rocks, expanding the current knowledge of the coastal aquifer system. A review of existing data was carried out, consisting of 307 borehole logs from 13 municipalities inside the area of interest, as well as 19 vertical electrical soundings and 37 logs from oil and coal exploratory drillings, that resulted in 315 input points for the model. This work builds up on the conceptual model previously developed for the area, that defined four hydrostratigraphical units for the region, and was able to constrain the geometries of the main aquifers (unit 1 and 3) and aquitards (unit 2 and 4) and their relation to the basement rocks, showing them to be more heterogeneous in thicknesses and extent than previously thought. In addition, this work was able to model what could be a fifth hydrostratigraphical unit, that strongly differs from the other four and could be an indication of the alluvial fans previously described in the literature.

Keywords Coastal aquifer system · Hydrostratigraphy · 3D modeling · GemPy · Brazil

Introduction

While coastal aquifers represent an important resource for populations living near the sea, their exploit has been growing significantly in the last decades leading to quality and quantity problems all over the world. Coastal areas tend to be more densely populated than the hinterland and exhibit higher rates of population growth and urbanization (Neumann et al. 2015). This leads to increased water use, and, if sustainable aquifer management is not implemented, also to depletion, contamination, and salinization of fresh groundwater (Bocanegra et al. 2010). Management of coastal aquifers becomes even more complex when considering that coastal areas will be the most affected by projected global sea-level rise (Kopp et al. 2014), both by its direct effects (i.e. high-tide flooding, salt-wedge migration) and indirect components (i.e. groundwater inundation—Habel et al. 2019). Considering that one of the greatest challenges in coastal aquifer management is the lack of awareness of

✉ Alexander Jüstel
alexander.juestel@ieg.fraunhofer.de

¹ Department of Geosciences, Federal University of Santa Maria (UFSM), Santa Maria, Rio Grande do Sul 97105-900, Brazil

² Geological Institute, RWTH Aachen University, 52062 Aachen, Germany

³ Fraunhofer Research Institution for Energy Infrastructures and Geothermal Systems IEG, Fraunhofer IEG, 52062 Aachen, Germany

⁴ Geological Survey of Brazil (SGB – CPRM), Criciúma, Santa Catarina 88802-010, Brazil

⁵ Institute of Hydraulic Research (IPH), Federal University of Rio Grande do Sul (UFRGS), Porto Alegre, Rio Grande do Sul 91509-900, Brazil

⁶ Polar and Climatic Center (CPC), Federal University of Rio Grande do Sul (UFRGS), Porto Alegre, Rio Grande do Sul 91509-900, Brazil

decision-makers and users regarding aquifer over-exploitation and contamination (Bocanegra et al. 2010), and more recently, regarding changes in coastal dynamics due to projected sea-level rise—finding ways of raising this awareness is essential for long-term planning of groundwater resources in those regions.

The coast of Rio Grande do Sul (the southernmost state of Brazil), is extremely susceptible to changes in sea level as it consists of an extensive and low-elevation plain with a complex system of lagoons (Da Silva et al. 2020; Dillenburg et al. 2005). The northern part of this coast is composed of 23 municipalities, that exhibited a high rate of population growth (25%) in the last 12 years (2010–2022), from approximately 340,000 to 425,000 inhabitants—mainly in the municipalities closer to the shoreline (IBGE 2022). The Northern Coast of Rio Grande do Sul is also a frequent touristic destination during the summer months (December–February), when total population increases by around 140%, even reaching 250% (more than 750,000 inhabitants) during specific holidays such as new year and carnival celebrations (Zuanazzi and Bartels 2016).

In this region, surface water is used for public supply, industrial and mixed uses, but mostly for irrigation of crops during the summer months of November to February. Still, for public water supply, 11 of the 23 municipalities rely exclusively on groundwater and another 6 have a hybrid system that rely between 20 and 75% on groundwater (ANA 2021). This indicates that for 74% of the municipalities, groundwater is a strategic resource in use. The number of inhabitants supplied with groundwater in the region might increase in the near future, though, considering the reliability of groundwater compared to surface water, specially in a scenario of a changing climate (Hirata and Conicelli 2012).

Regardless of an increase in groundwater exploration in the area, the current situation already demands improving groundwater management. Today, even the cities with the highest fixed and seasonal populations in the region—Capão da Canoa, Tramandaí, Osório and Torres—have low rates of sewage collection (with or without treatment): 16%, 15%, 41% and 44%, respectively, and are mostly dependent upon in-situ solutions such as septic tanks (Brasil 2023). Thus, there is a significant pollution potential of the unconfined aquifer with bacteria and nitrate, and even the confined aquifer might be affected due to irregular and badly-constructed wells, or due to wells screening multiple layers, a common practice in the region (Troian et al. 2020). Land use practices in agriculture might add up to diffuse pollution caused by in-situ sanitation, a type of pollution that can not be addressed directly by environmental legislation but requires definition of specific policies (Foster and Chilton 2021).

Despite efforts from the hydrogeologic community, groundwater traditionally receives far less attention than

surface water (Famiglietti 2014). Undervaluing groundwater in water policies and limited groundwater knowledge are amongst the key causes of unsustainable groundwater management (Mahlknecht and Mora 2022). To this date, no serious problems of scarcity, salinization, or any other type of contamination in the region's aquifers have been reported, and so, empiricism prevails in groundwater management (Collischonn and da Camara Rosa 2022). But as the population and the vulnerability to sea-level rise increases (Da Silva et al. 2020), so does the pressure in the region's aquifers, suggesting the need to expand the knowledge of groundwater resources on the Northern Coast of Rio Grande do Sul and to convey this geoscientific information to the society and decision makers—aiming to improve aquifer management. Nonetheless, communication with those actors should be carried out using effective ways of transmitting knowledge—which might not mean, necessarily, using the most technical language, as those actors will have varying backgrounds that might or might not include groundwater expertise.

One useful tool for effectively communicating geological information is the visual representation of data using three-dimensional (3D) modeling (Campbell et al. 2017; Terrington et al. 2008). Three-dimensional structural geological models are geometric representations of our (limited) knowledge of relevant subsurface geological features and structures (De La Varga et al. 2019; Wellmann and Caumon 2018), and are useful both for specialists and non-specialists alike: to the former, it can help in the assessment of existing data and major structural features, which in turn supports future data-gathering campaigns and conceptual model development and improvement (Scott et al. 2019), as well as serve as a basis for subsequent hydrogeological modeling and simulations; to the latter, it can help to visualize geoscientific information and understand its conceptual basis (Terrington et al. 2008). Basically, 3D geological models can help closing the knowledge gap between 'subsurface experts' and potential users of subsurface knowledge (Campbell et al. 2017).

Three-dimensional geological models representing hydrostratigraphical units and their horizontal and vertical variations are also useful to the development of a sound groundwater conceptual model (Enemark et al. 2019), as aquifer dynamics, groundwater flow, and the effects of hydrologic changes in the aquifer system can only be understood by first delineating and describing the aquifers and confining units (Winner and Coble 1996). Furthermore, an accurate hydrostratigraphical model is key in the eventual development of a numerical groundwater model – a computer-based representation of the essential features of a natural hydrogeological system, designed to provide insights into complex system behavior and dynamic

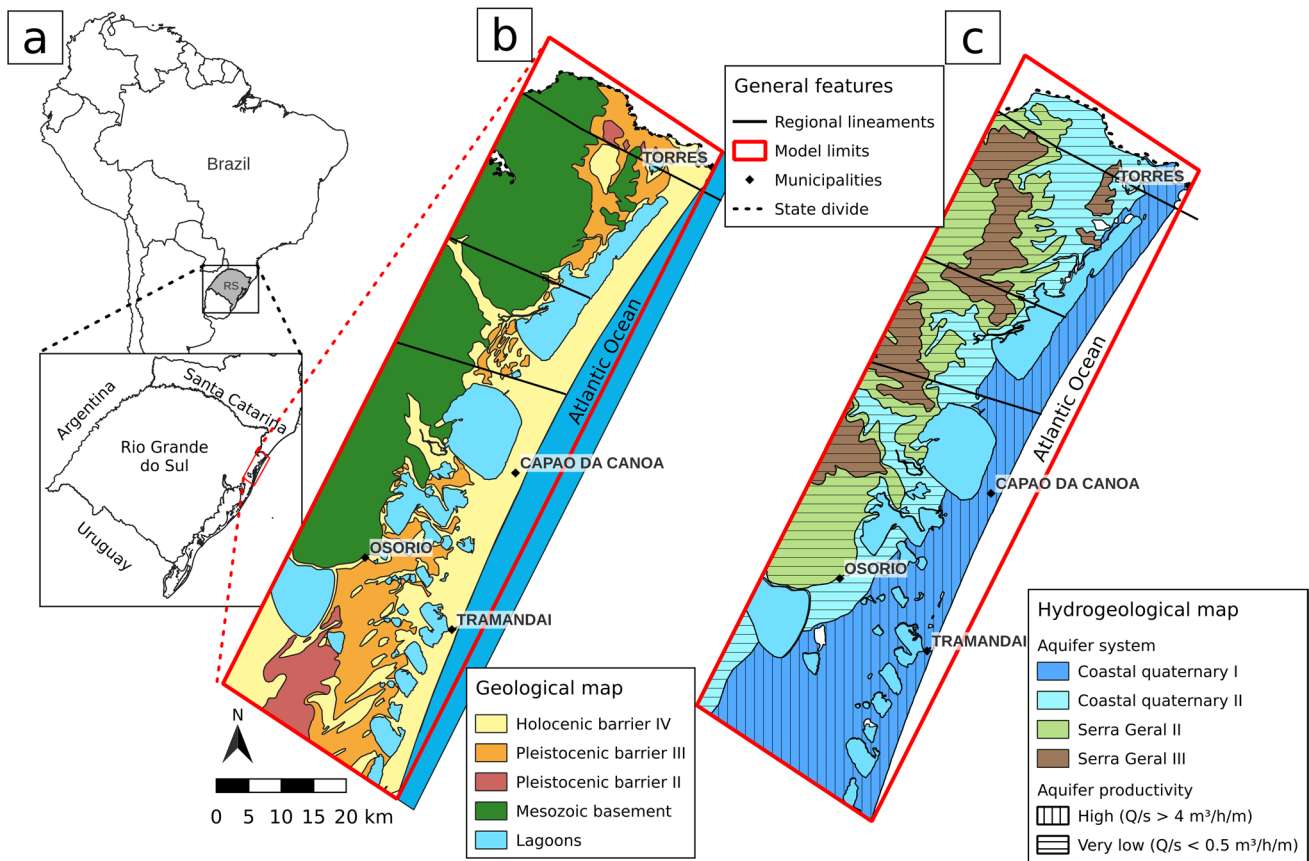


Fig. 1 a Location of the Northern Coast of Rio Grande do Sul (RS) in the country and state map. b Simplified geological map of the Northern Coast of RS. c Simplified hydrogeological map of the Northern

Coast of RS. Source data from Viero et al (2009); Machado and Freitas (2005) and Wildner et al. (2008)

conditions—as the accuracy of a numerical groundwater model is directly related to the quality of the input data (Åberg et al. 2021; Kumar 2013).

In order to contribute to the refinement of the hydrogeological understanding of the Northern Coast of Rio Grande do Sul and to share this knowledge with various stakeholders of the society, a 3D hydrostratigraphical model of the region is presented in this work. Our aim with this model is to integrate all available data and to identify areas that need further investigation and better understanding. This model was built using the free, robust, and open-source Python-based geomodelling library GemPy (De La Varga et al. 2019), based on the principles of easy access and free usability (Campbell et al. 2017; Dramsch 2020; Kinkade and Shepherd 2022; Mader and Schenk 2017), so academics, non-government organizations, and other decision- and policy-makers can use it for their own needs. This model is based on the existing hydrostratigraphical conceptual model developed by Troian et al. (2020). All users are welcome to contribute to it, either by improving its code or by producing and sharing data to be integrated into it, in the light of open collaboration networks (Mergel 2015).

Geological and hydrogeological context

The area of interest (AOI) of this study is delimited by the four following vertices, in decimal degrees: (1) $-29.150789^{\circ}/-49.982469^{\circ}$; (2) $-29.309031^{\circ}/-49.704233^{\circ}$; (3) $-30.217021^{\circ}/-50.217954^{\circ}$; (4) $-30.058022^{\circ}/-50.497625^{\circ}$ (or in UTM zone 22 J, EPSG 31982: (1) 598,966 m E/6,774,880 m S; (2) 625,836 m E/6,757,079 m S; (3) 575,263 m E/6,656,908 m S; (4) 548,425 m E/6,674,679 m S) (Fig. 1). The AOI is a rectangular area of 32×112 km, or 3.584 km², and encompasses 14 of the 23 municipalities of the Northern Coast of Rio Grande do Sul state: Arroio do Sal, Capão da Canoa, Cidreira, Dom Pedro de Alcântara, Imbé, Mampituba, Maquiné, Morrinhos do Sul, Osório, Terra de Areia, Torres, Tramandaí, Três Cachoeiras and Xangri-lá.

To the northwest/west part of the AOI, the Mesozoic rocks of the São Bento Group (Paraná Province) crops out (Wildner et al. 2008), and constitute the basement, in this area, of the unconsolidated sediments of the Pelotas Basin. The Pelotas Basin was formed during the fragmentation of the Gondwana continent and the opening of the South Atlantic, and is described in detail in (Rosa et al. 2017).

The coastal plain of Rio Grande do Sul state, where the AOI is located, is a physiographic feature of the upper, onshore part of the Pelotas Basin (Rosa et al. 2009), and is divided into an alluvial fan system and four barrier-lagoon systems (Tomazelli and Villwock 2000). The alluvial fan system is of Tertiary age, and developed adjacent to the outcropping rocks of the São Bento Group as a result of the erosion and transport of its sediments. Above this fan system and in a progressively lower sea level trend, four barrier-lagoon systems, from four different transgressive–regressive cycles, were deposited (Villwock 1984). Those barrier-lagoon systems deposited during the Pleistocene and Holocene, as a result of climatic variations and glacio-eustatic oscillations, and are named according to their age, three of them being Pleistocenic I (325 ka), II (200 ka), III (125 ka) and the most recent, Holocenic IV (currently active) (Collischonn and da Camara Rosa 2022).

The sedimentary systems existing in the AOI gave origin to highly heterogeneous (vertically and horizontally) aquifers with different confinement levels (unconfined, semi-confined and confined, Troian et al. 2020). The hydrogeological map of Rio Grande do Sul (Machado and Freitas 2005) defines two main aquifers along the northern coast of the state: The Coastal Quaternary Aquifer System I (closer to the shore), with higher specific capacities ($> 4 \text{ m}^3/\text{h}/\text{m}$) and total dissolved solids (TDS) below $400 \text{ mg}/\text{L}$; and the Coastal Quaternary Aquifer System II (inland), with specific capacities ranging from low to medium (between 0.5 and $1.5 \text{ m}^3/\text{h}/\text{m}$) and TDS ranging from 600 to $2000 \text{ mg}/\text{L}$. Nonetheless, this division is not representative of in-depth, older geological units with distinct hydrogeological characteristics (Collischonn and da Camara Rosa 2022; Troian et al. 2020).

To acknowledge this in-depth variability, Troian et al. (2020) developed a hydrostratigraphical conceptual model detailing the vertical heterogeneity of the Coastal Aquifer System in the Northern Coast of Rio Grande do Sul—a significant contribution to the area’s groundwater knowledge—through the analysis and review of geological and constructive profiles of 107 water wells, 15 geophysical logs (natural gamma, electric resistivity, and sonic profiles) and water quality analysis (TDS). The authors defined four different hydrostratigraphic units related to Cenozoic deposits in terms of its granulometric composition, effective porosity, and TDS of the respective groundwater. A brief description of those four units can be seen in Table 1 and the conceptual model can be seen in Fig. 2. It is important to note that Troian et al. (2020) used the hydrogeologic taxonomy classification proposed by Diniz et al. (2014), which define a hydrostratigraphical unit as the less-constraining hierarchical class that does not necessarily correspond to the stratigraphical units of a region. This classification considers that a geological unit might present internal variations, in different scales, that affect its hydrogeological characteristics.

Based on the hydrostratigraphical conceptual model by Troian et al. (2020) and focusing on understanding the genesis of one specific unit of the Coastal Aquifer system (the ‘*Sal Grosso*’ unit, equivalent to Unit 3 in this work), Collischonn and da Camara Rosa (2022) carried out 19 vertical electrical soundings with a maximum investigation depth of 100 – 110 m below surface. The resulting geoelectric stratigraphy presented good correlation with the lithological profiles of drilled wells in the region and with the top three units defined by Troian et al. (2020), despite differences in layer thicknesses (which is expected, considering the heterogeneity and variations of the Coastal Aquifer System). Collischonn and da Camara Rosa (2022) interpreted the

Table 1 Brief description of the four main hydrostratigraphic units existing in the AOI, based on Troian et al. (2020)

Unit	Approx. depth	Thickness	Description	Hydraulic behavior
Unit 1	Surface	Usually between 15 and 30 m	Composed mainly of yellowish fine to medium sands and containing discontinuous clay lenses of variable thicknesses. Higher values of effective porosity and low salinity	Unconfined Aquifer
Unit 2	15–30 m below surface	Up to 45 m	Predominantly composed of gray-colored argillaceous sediments (clay and silt) with lenses of fine to very fine sands. Lower values of effective porosity and higher salinities	Aquitard
Unit 3 (Sal Grosso aquifer)	60–75 m below surface	Between 5 and 40 m	Composed mostly of medium to coarse sands with a few clay layers in between. Higher values of effective porosity and low salinity	Confined Aquifer
Unit 4	$> 75 \text{ m}$	Unknown	Consists mainly of gray and brown clay layers intercalated with fine sands. Lower values of effective porosity and higher salinities	Aquitard

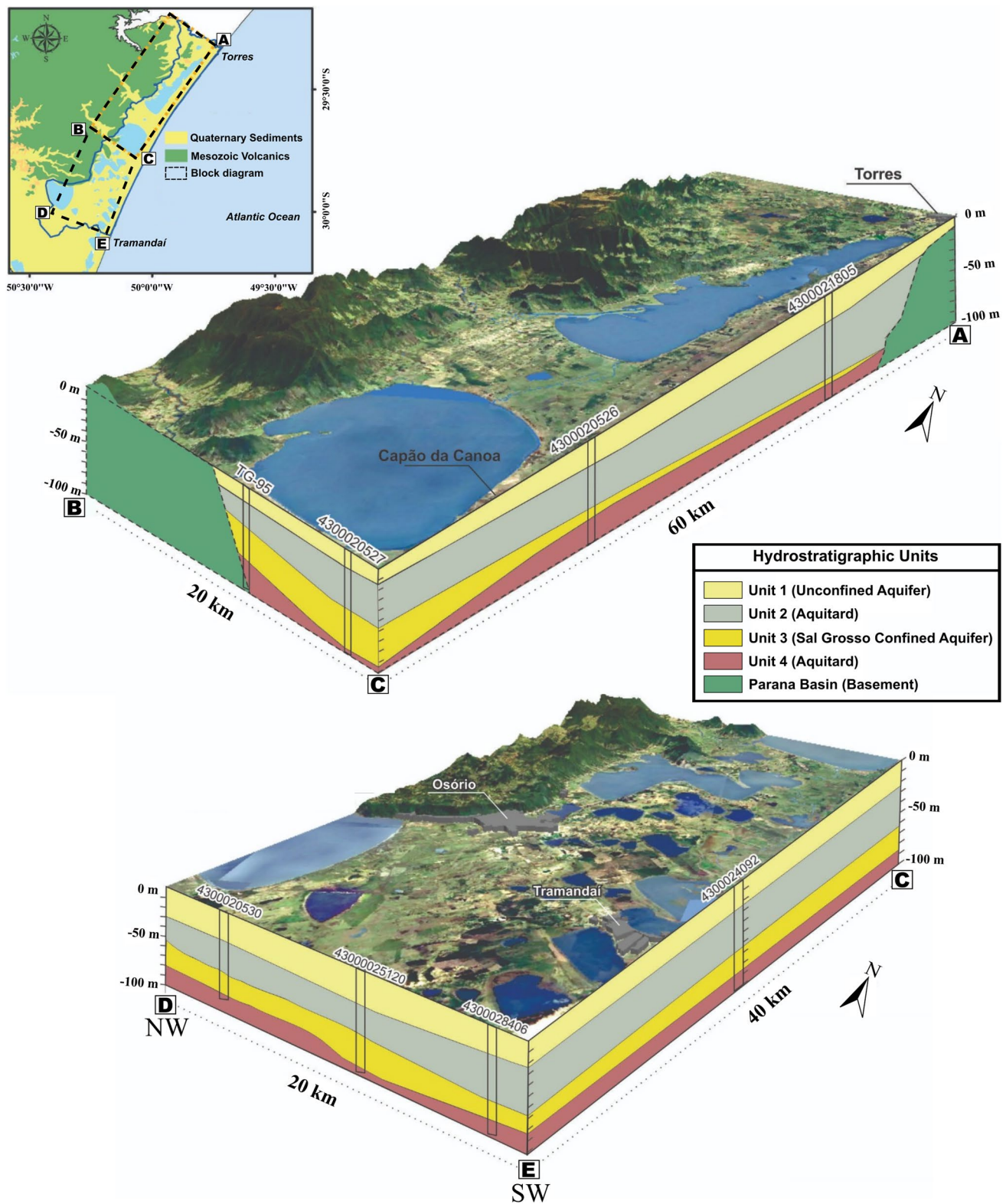


Fig. 2 Block diagram of the conceptual model built by Troian et al., (2020), with the distribution of the main hydrostratigraphic units in the AOI. Numbers in the diagrams (e.g. TG-95) indicate drilling logs used for the work

confined ‘*Sal Grosso*’ aquifer to be an elongated feature in the NW–SE direction, perpendicular to the current coastline, constituting a paleochannel responsible for the transport of sediments from the granitoid rocks of the Sul- Riograndense Shield (further west and outside the AOI), associated with the paleodrainage system of the Jacuí River.

Materials and methods

Data acquisition

The first step of this work was gathering existing geological and hydrogeological information of the AOI and the existing division of hydrostratigraphical units. This step relies on the findings and data from Troian et al. (2020) and Collischonn and da Camara Rosa (2022), as those are the most recent and comprehensive works carried out in the AOI focusing on hydrostratigraphy. Additionally, three main datasets were reviewed: (1) 307 borehole logs from water wells drilled in the 14 municipalities of the Northern Coast of Rio Grande do Sul, kept by the Geological Survey of Brazil (SGB-CPRM) and freely available in the Brazilian Groundwater Information System (SIAGAS – CPRM., 2023); (2) two logs from the national oil exploration and production database (*Banco de Dados de Exploração e Produção* – BDEP – ANP, 2023); (3) A database of 35 drilling logs of a coal exploratory project (here named as CEP) carried out by SGB-CPRM in the early 1980s, 22 of them with natural gamma profiles. The geographic distribution of points from all datasets can be observed in Fig. 3.

Geoprocessing and data preprocessing

The free and open source software QGIS (QGIS.org, 2023) was used in this project as the main geographic information system (GIS) tool for spatial analysis of data, elaboration of maps and preprocessing ‘surface’ and ‘orientation’ points which were then used as input for the 3D model (see “[Three-dimensional modeling](#)”). Figures were also drawn in QGIS and adjusted in Inkscape (Inkscape.org) using Coblis (colorblindness.com/coblis-color-blindness-simulator/) as a support for choosing best color composition. GemGIS (Jüstel et al. 2022), a Python-based, open-source geographic information processing library, was used to create depth maps of the surfaces modeled. A digital elevation model (DEM) of the area was also used in this work, obtained from the TopoData project (Valeriano and Rossetti 2012), a free source kept by the Brazilian National Institute for Space Research (*Instituto Nacional de Pesquisas Espaciais* – INPE). The TopoData project refines and post-processes data from the Shuttle Radar Topography Mission (SRTM), increasing its resolution from 3 arc seconds (90 m) to 1 arc second (30 m)

using kriging techniques over the entire Brazilian territory (Valeriano and Rossetti 2012). Raw data management was carried out using LibreOffice Calc.

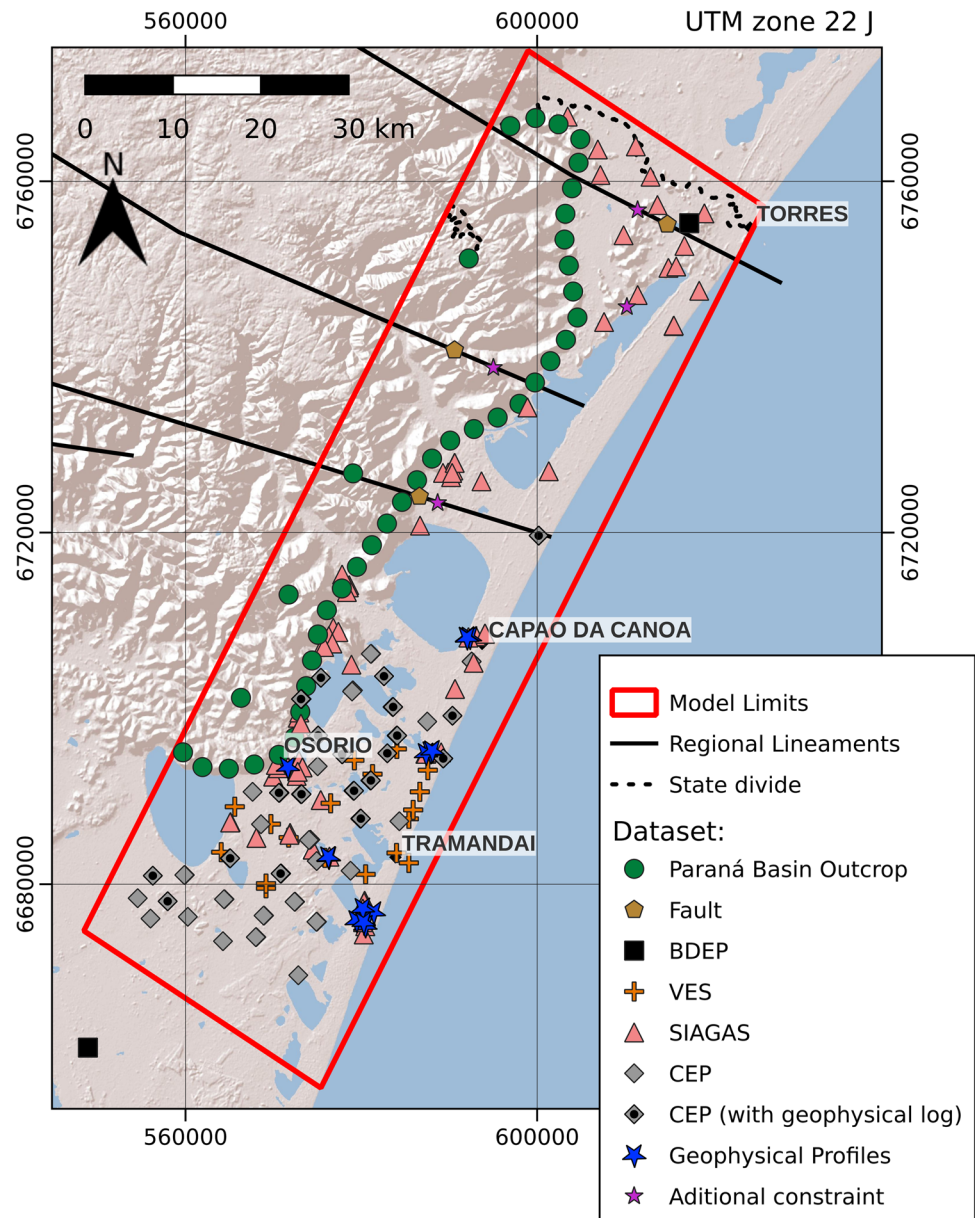
Three-dimensional modeling

The three-dimensional hydrostratigraphical model of the AOI was created using GemPy (De La Varga et al. 2019), a full open-source geomodeling algorithm based on an implicit potential-field interpolation approach developed by Lajaurie et al. (1997) and based on the mathematical principles of universal cokriging (Chiles and Delfiner 2009). GemPy uses the potential-field approach as the central method to generate the models, and implements it via the programming language Python. GemPy is capable of constructing complex full 3D geological models and provides a basis for open scientific research using geological models, with the aim to foster reproducible research in the field of geomodeling (De La Varga et al. 2019).

Although GemPy has a series of assets for advanced scientific investigations, such as integration with machine-learning, Bayesian inference frameworks (De La Varga and Wellmann 2016), stochastic geological modeling, inversions (Güdük et al. 2021), model topology analysis (Brisson et al. 2023; Schaaf et al. 2021) computation of gravity fields (De La Varga et al. 2019), and hydrogeological heterogeneity characterization (Thomas et al. 2022), the core aspects of its functionality are simple for the final user. One can compute a 3D visual representation of an area by using the basic functions of GemPy: by loading a ‘comma-separated values’—CSV file containing a list of ‘surface’ and ‘orientation’ points with coordinates, a Z value (depth) of a layer above or below mean sea level, and the dip and azimuth of that respective layer at an accessible point; assigning each data point to its respective geological formation; then setting the relationship between those formations. In GemPy, all the input data has to be referred to a surface, and a surface always marks the bottom of a unit, so the Z values added correspond to the bottom of a formation, not the top. Surfaces are then assigned to a series: series can have as many surfaces as needed. A potential field is calculated for each series and one surface is equal to the isovalue of the scalar field, while the provided orientations define the gradient of the scalar field. Multiple parallel to subparallel layers can be modeled in one series using one scalar field, and the offset of faults is calculated automatically using a drift function (De La Varga et al. 2019).

For the definition of the hydrostratigraphical units, this work follows Troian et al. (2020). Thus, units are labeled, from surface to depth: Unit 1; Unit 2; Unit 3 and Unit 4. The definitions of Unit 1, Unit 2 and Unit 3 from Troian et al. (2020) correspond, respectively, to Unit 3, Unit 2 and Unit 1 identified by Collischonn and da Camara Rosa (2022)—the

Fig. 3 All data points used in this work, discriminated by data type. “Geophysical Profiles” indicate the 15 geophysical logs (natural gamma radiation, electric resistivity, and sonic profiles analyzed by Troian et al. (2020)); “VES” indicates the location of the 19 vertical electrical soundings carried out by Collischonn and da Camara Rosa (2022); “BDEP”, “CEP” and “SIAGAS” datasets are described in “Data acquisition”; “Fault”, “Paraná Basin Outcrop” and “Additional Constraint” are described in “Three-dimensional modeling”



former starts counting from the surface and the latter from depth. A fifth unit named ‘Pelotas_Basin_Lower’ was added, to represent the lower part of the Pelotas Basin in the area, consisting mostly of alluvial fan deposits, with the bottom identified in three CEP points and two SIAGAS. The model also has a series “Parana Province” and “Basement”.

The first draft of the model, in the beginning of our works, was constructed using only data from Troian et al. (2020) and relying on his interpretation of the hydrochemistry, lithologic and geophysical profiles available for the area. In a second step, we added the VES data from Collischonn and da Camara Rosa (2022), and thus built the model first using the most reliable data available in order to develop a solid understanding of the AOI. Then, the datasets described in “Data acquisition”. ‘Data acquisition’ (SIAGAS, CEP,

BDEP) were reviewed, and logs of interest were used as input data. Drilling logs were selected when limits between hydrostratigraphical units were deemed clear, based on each unit’s characteristics as described in Troian et al. (2020): based on lithology, color, grain size, expected depths and relation between units. Logs were discarded as incongruous data if profiles were absent or inconclusive. In fact, from the total 344 logs reviewed, only 139 presented at least one surface point and could be used as input data—102 from SIAGAS, all 35 logs from CEP and the 2 from BDEP. This suggests an absence of a technician/geologist present during the drilling of those remaining 205 boreholes from SIAGAS, leading to lack of profile logging. Figure 4a shows the distribution of used logs and incongruous data in the area

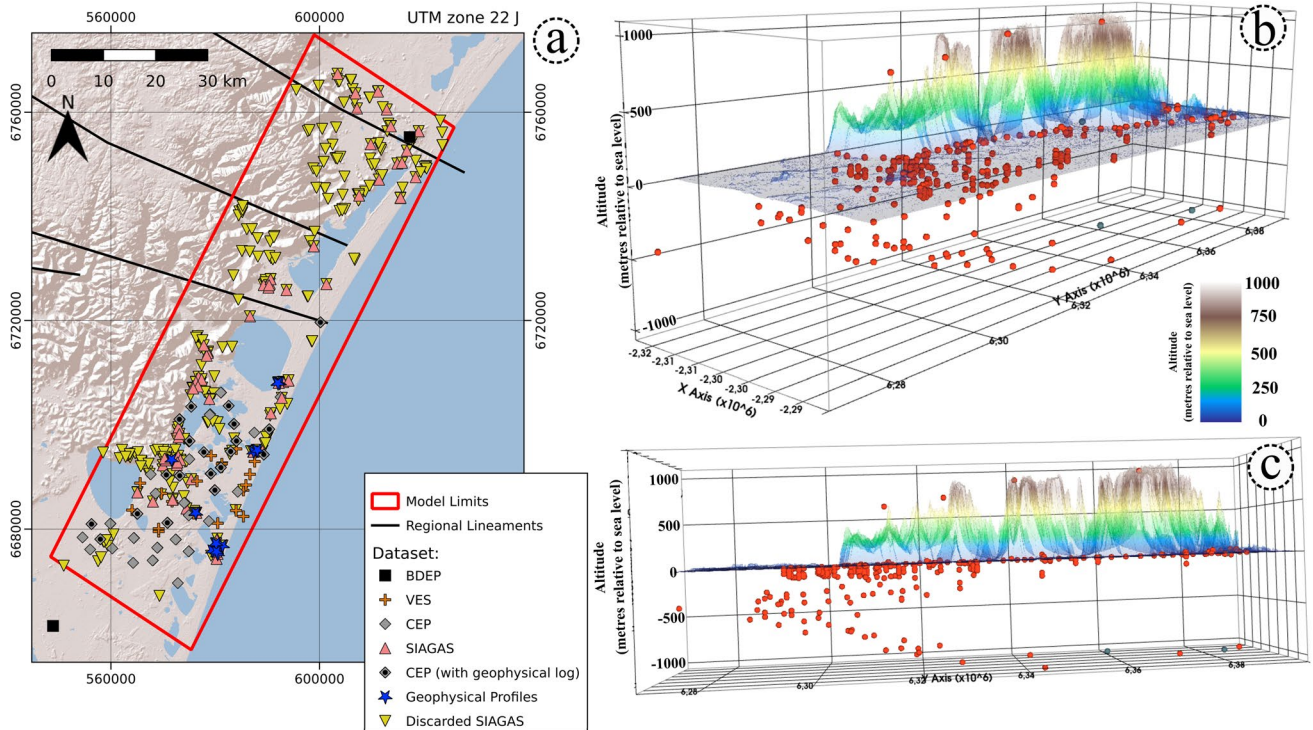


Fig. 4 a Geographical distribution of data reviewed for this work, discriminating the ones used as input points (102 from SIAGAS, all 35 logs from CEP and the 2 from BDEP) and the discarded as incongru-

ous data (205, all from SIAGAS). b and c Point distribution in depth with DEM topography shown. Point of view is from south to north in 'b' and southwest to northwest in 'c'

map, while Fig. 4b and c show distribution of used points in depth.

The process of reviewing the geological logs is exemplified in Fig. 5 (in a simplified way for explanation purposes): the drilling log (1) shows a transition of (yellow) sands on top; (gray) fine sediments; medium/coarse sands; (gray/brown) fine sediments and at the base of the borehole an intercalation of (mostly) sands. In this log, it was possible to define the base of Units 1, 2, 3 and 4, and thus four data points were generated for GemPy. Drilling log (4), though, did not present a conclusive transition between units, and thus did not generate input points. Some of the vertical electrical soundings (VES) profiles from Collischonn and da Camara Rosa (2022) required a slightly different approach, as the bottom of the units were not reached but the model was underestimating layer thicknesses if those points were not added (VES 2, 3, 6, 8, 10, 11, 16, 17, 18 and 19—see “Comparing Unit 3 extension with previous works” for location of those points). In those cases, we used the profile depth (~100–110 m) as the bottom of the unit. This approach has obvious limitations, described in detail in “Model limitations”.

To observe the hydrostratigraphical units in different Z scales, the data was modeled in three details: first the whole depth of the Pelotas Basin, Paraná Basin and the

Precambrian basement (down to 1200 m below sea level—Model 1), then a detailed view of the top 150 m (focusing on Unit 1, 2, 3 and top of Unit 4—Model 2) and then the whole depth of the Pelotas Basin (~530 m—Model 3). Those are presented in “Modeling the Paraná Basin and the Precambrian basement (Model 1)” and “Modeling the Pelotas Basin” of this work. The models were computed and ran several times on a trial-and-error approach using resolutions (X, Y, Z) starting with 70, 70, 70 and improved to 128, 400, 120 when the model was well established. The dataset was manually adjusted when needed (i.e. keeping depths and coordinates untouched but changing dip and azimuth of points) to better represent the known geology and correct for artefacts—this manual adjustment was done specifically for the basement and Parana Province only, as the unconsolidated sediments from Unit 1 to 4 were considered to be close to horizontal. Here, “resolution” means the number of cells spread across the model extent, which causes the voxel size to differ in every direction.

To represent the outcropping of the Paraná Province in the west/northwest of the AOI, 40 interface points were added, obtained by analyzing the DEM and the geological map, in QGIS. Three regional, high angle faults (85°), were also represented in the model by adding surface and orientation points at an elevation of 0 m and manual

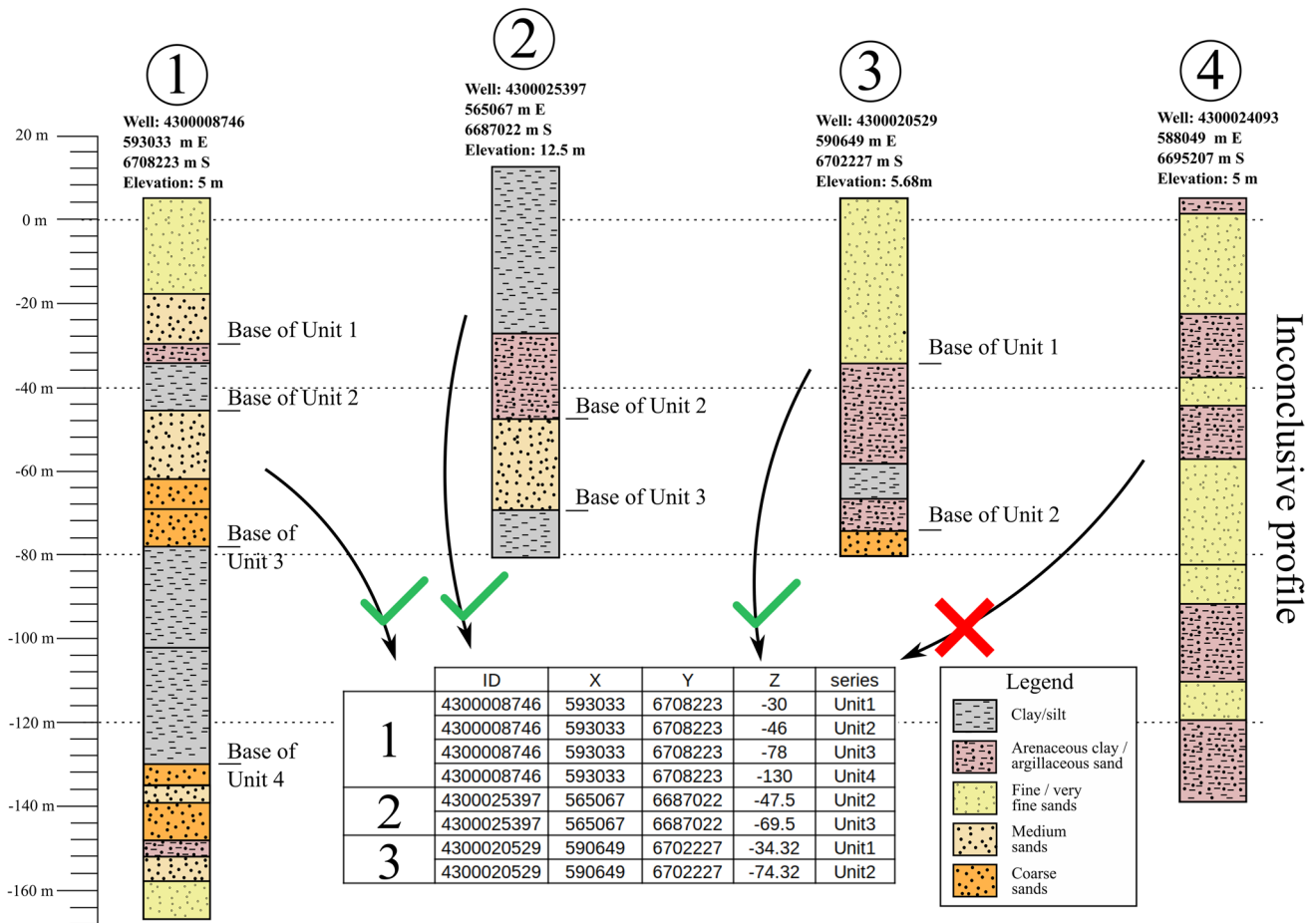


Fig. 5 Simplified example of the process of reviewing the original datasets and creating the GemPy input file. In this example, four SIAGAS wells were used, each with different lithological variations.

While wells (1), (2), and (3) presented profiles that allowed defining the base of specific units, well (4) presented an inconclusive profile and was not included in the input file

additional constraints (no real data) at – 1000 m, inferred based on location on the surface, azimuth and dip of each fault. Those faults cross the Paraná Basin and the Precambrian basement and are associated with the Terra de Areia – Posadas fault system (Machado and Faccini 2004; Philipp et al. 2014; Wildner et al. 2008). One additional manual additional constraint (no real data) was added for the interface between the Precambrian basement and the Paraná Basin at a depth of – 1000 m in the northeast of the AOI, because the model was unable to compute the basement between faults unless at least one point of data was added. At last, two manual constraints were added along the SW and NE boundaries of a layer of alluvial fan deposits, identified in a specific area of the Pelotas Basin, to correct an artefact caused by the layer geometry; those two points are a copy of two real data points (4,300,024,097—SIAGAS and GT-007-RS-CEP) but were plotted 1 m apart of the original points and had their orientations (azimuth and dip) changed to restrain the geometry. Those six

manual additional constraints (three for the faults, one for the basement and two for the alluvial fan layer) are labeled accordingly in the dataset.

Table 2 shows the main parameters of the models developed in this work. The links to the dataset, as well as to the full code and the required packages list and versions (.yml file) are available at the end of this document in “Data availability and code”.

Results

Modeling the Paraná Basin and the Precambrian basement (Model 1)

The 3D model generated by GemPy for the area basement and its interface with the Pelotas Basin can be observed in Fig. 6 and in three 2D sections of it in Fig. 7. The

Table 2 Main parameters of the models developed in this work

Parameter	Model 1	Model 2	Model 3	Unit	Source
	Value				
Coordinate Reference System (CRS)	EPSG: 31982			–	One of the CRSs for the area
xmin	548.425			m	Geological setting
xmax	625.836			m	Geological setting
ymin	6.656.908			m	Geological setting
ymax	6.774.880			m	Geological setting
zmin	– 1.200	– 150	– 530	m a.s.l	Geological setting
zmax	50	20	20	m a.s.l	Geological setting
Model extent (width x length)	32 × 112			km	
Model extent (area)	3.584			km ²	Geological setting
Model extent (volume)	4.480.000	609.280	1.971.200	km ³	Geological setting
Model resolution (cells per direction)	128/400/120	128/400/80	128/400/50	cells	Hardware limitations
Model resolution (total cells)	6.144.000	4.096.000	2.560.000	cells	Hardware limitations
X	250			m/cell	Hardware limitations
Y	280			m/cell	Hardware limitations
Z	10,4	2,1	11	m/cell	Hardware limitations
Interface points	159	315	315	points	Input data
Orientations	159	315	315	points	Input data

Model 1 focused on the Paraná Basin and the Precambrian basement (down to 1200 m below sea level); Model 2 focused on the top 150 m of the Pelotas Basin in the AOI; Model 3 focused on the whole depth of the Pelotas Basin (~ 530 m below sea level)

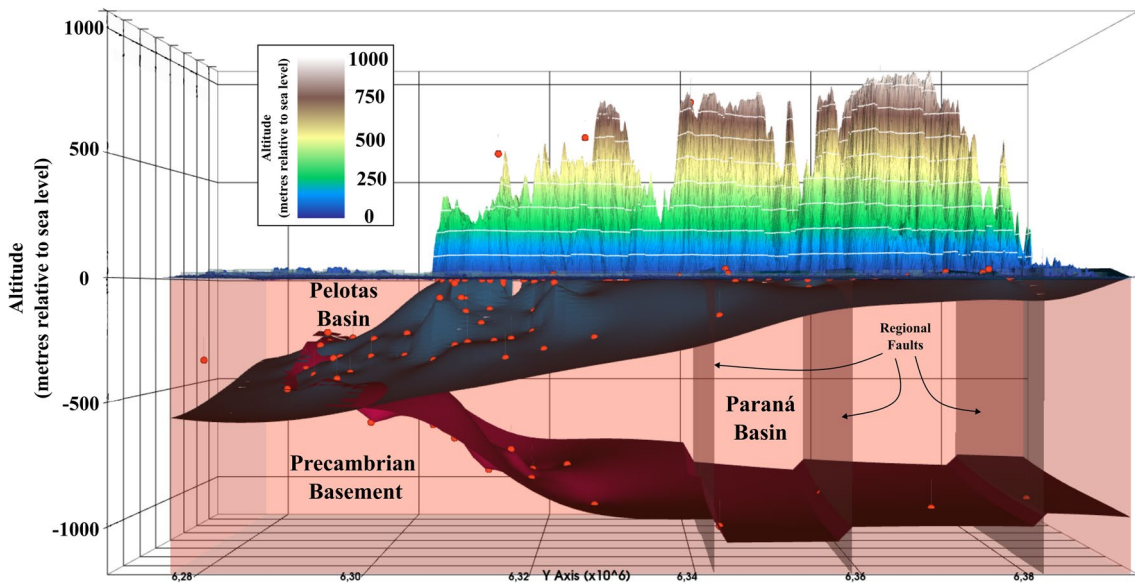


Fig. 6 Three-dimensional model of the basement of the area (Precambrian and Paraná Basin rocks) and their interface with the Pelotas Basin. Red surface: top of Precambrian rocks; blue surface: top of the Paraná Basin; gray surfaces: regional faults. Vertical exaggeration: 30x

Precambrian basement is identifiable in 29 drilling logs in (or close to) the AOI: in two logs from the BDEP dataset (2TO0001RS and 2PS0001RS) and in 27 of the CEP dataset; depths of its top vary from 317 to 1066 m below sea level. The shallower depths are located in the southwest of the area, while the deepest point to the top of

the basement is in the central region of the AOI. Most points are concentrated in the central-to-southwest-region of the AOI, with only one point in the central region and another in the northeast. The Paraná Basin was observed in 84 drilling logs: in the same two logs from the BDEP dataset, in 35 logs from the CEP and, due to its proximity

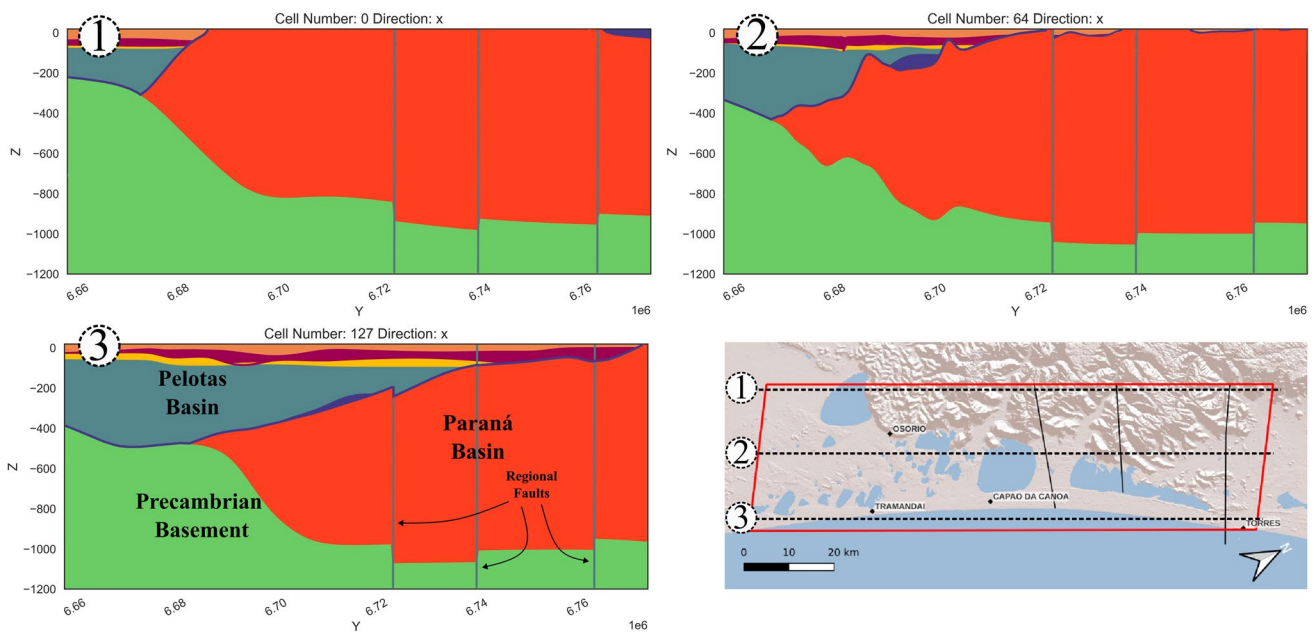


Fig. 7 Cross-sections of the AOI modeled basement (Precambrian and Paran Basin rocks) and their interface with the Pelotas Basin

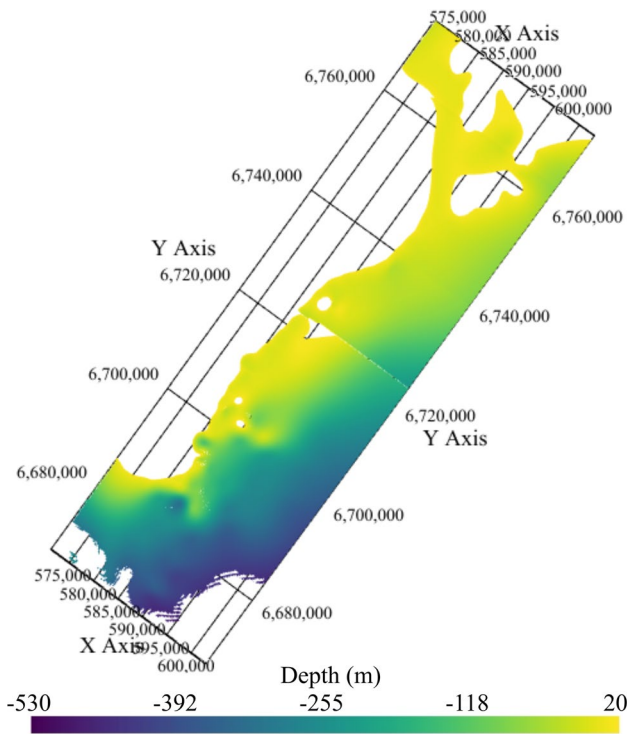


Fig. 8 Depth map of GemPy-generated interface between the Pelotas Basin and its basement (Paran Basin and Precambrian rocks). Blank areas to the west, northwest and north are Paran Basin outcrops above 20 m of altitude (outside model scope)

to the surface and outcropping regions, also in 45 logs from borehole drillings (SIAGAS database). The greatest depth observed to the top of the Paran Basin (or the base of the Pelotas Basin) was ~ 550 m below sea level, in the south of the AOI, with the basin getting thicker and the top getting shallower to the northeastern part of the AOI. In Fig. 8, one can see the depth of the interface between the Pelotas Basin and its basement, showing that most of the basin in the AOI is relatively shallow (< 250 m below sea level).

Modeling the Pelotas Basin

The AOI presents abundant data from existing borehole drillings down to ~ 100–150 m (Collischonn and da Camara Rosa 2022; Troian et al. 2020), allowing a more robust representation of the top units comparing to the lower sections of the model. In total, the Pelotas Basin was identified in 139 points of the datasets: 80 from SIAGAS; 2 from BDEP; 38 from CEP, and in the 19 VES from Collischonn & da Camara Rosa (2022). Most of those 139 points generated more than one input point for GemPy, as the boundaries of more than one hydrostratigraphical unit were identified in each, as shown in Table 3.

Although there are sections of the AOI with few input points, GemPy was able to model them by using the

Table 3 GemPy input points of each unit of the Pelotas Basin in the AOI, respective to each dataset reviewed

Dataset Unit	SIAGAS	BDEP	CEP	VES	Total input points in GemPy
Unit 1	36	0	1	19	56
Unit 2	37	0	1	19	57
Unit 3	33	0	1	1	35
Unit 4	1	0	4	0	5
Pelotas Basin lower	46	2	37	0	85

Note again that GemPy uses the bottom of units as input, and thus points were added only when the data fulfilled this requirement (e.g. Unit 3 was identified in several VES profiles, but bottom of unit only in one)

geometry of other surfaces (units) surrounding and constraining them, due to the implemented potential field, where parallel layers can be modeled using one scalar field (De La Varga et al. 2019). This is the case for the alluvial fan deposits existing in parts of the Pelotas Basin (unit named here as ‘Pelotas Basin Lower’). The boundary between Unit 4 and ‘Pelotas Basin Lower’ was observed only in five drilling logs, but the unit’s geometry was modeled successfully because: (1) the bottom of ‘Pelotas Basin Lower’ was well delimited by several input points, visible in the logs as a stark change in geology, from Cenozoic sediments to the volcanic/sedimentary rocks of the Paraná Basin; (2) the logs where the alluvial fan deposits occur are contiguous, allowing the representation of a geometry; and (3) the bottom of Unit 3 (and thus the top of Unit 4) is well delimited and consistently (nearly) horizontal along the AOI.

Units 1, 2 and 3 are restricted to the top 100 m of the Pelotas Basin, while Unit 4 represents the biggest volume of sediments in it—with thicknesses up to 470 m and maximum depth of 530 m, reaching the base of the basin in the AOI. Thus, we opted to present here two subsections of the model results: first a detail of the top 150 m (focusing on Unit 1, 2, 3 and top of Unit 4) and then the whole basin depth (~ 530 m).

The top 150 m (Model 2)

The 3D model generated by GemPy for the top 150 m of the Pelotas Basin in the AOI is presented in Fig. 9, while Fig. 10 shows three 2D sections of the area and Fig. 11 shows depth maps of the modeled interface surfaces. Looking at the top 150 m of the model, it is possible to observe that Unit 1, 2 and 3 present varying thicknesses along the AOI—Unit 1 and 3, the main aquifers of the AOI do not present a regular geometry and the latter is discontinuous. Unit 1 presents a maximum thickness of 40 m, going to depths of – 40 m below sea level, but in the southern part of the AOI was modeled as absent; Unit 2 crops out in parts of the AOI, and can be as thick as 90 m and as thin as 10 m, but tends to present a more regular geometry than Unit 1. Unit 3 presents maximum thicknesses of around 25–30 m, computed in the southeast of the model, gets thinner towards northeast and is absent in the southwest and central parts of the AOI. Unit 4 appears on the model at depths of around 50 m and below, and at those depths another unit was observed, that will be detailed later in this work “[A Fifth Unit](#)”.

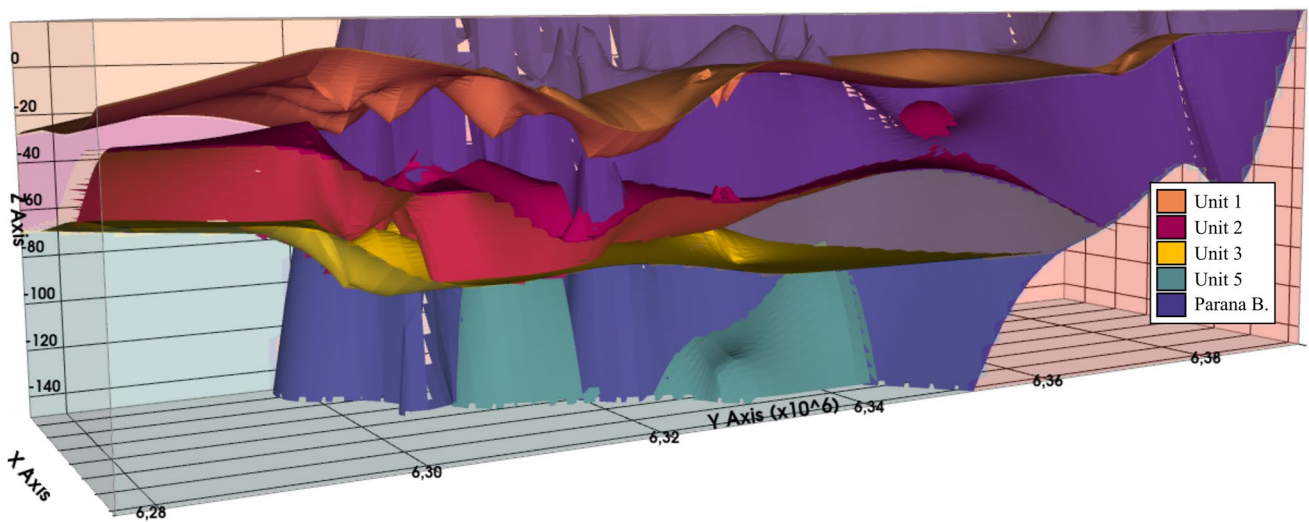


Fig. 9 Top 150 m of the Pelotas Basin model in the AOI showing the bottom surfaces of Unit 1, Unit 2 and Unit 3. Note that Unit 4 is not shown in the legend as it corresponds to all volume below Unit 3. Unit 5 will be detailed in “[A Fifth Unit](#)”. Vertical exaggeration: 200x

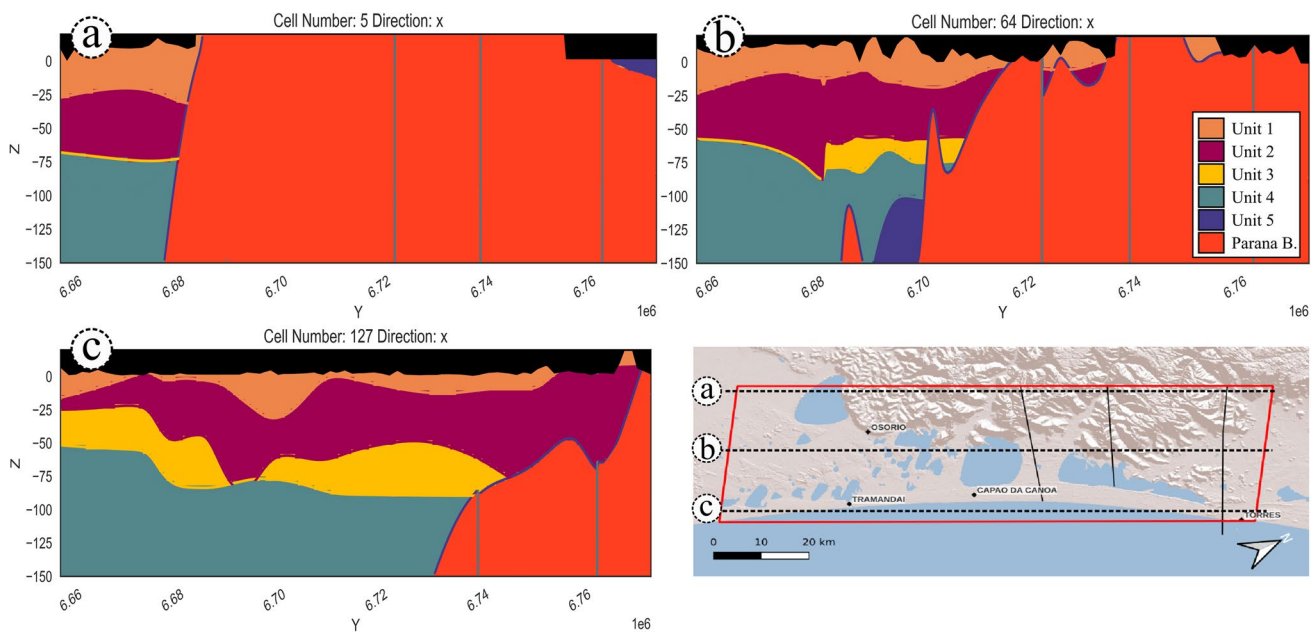


Fig. 10 Cross-sections of the top 150 m of the modeled Pelotas Basin in the AOI. The interface between Unit 1 and the black area in (a), (b) and (c) is the area's topography. Vertical exaggeration: 200x

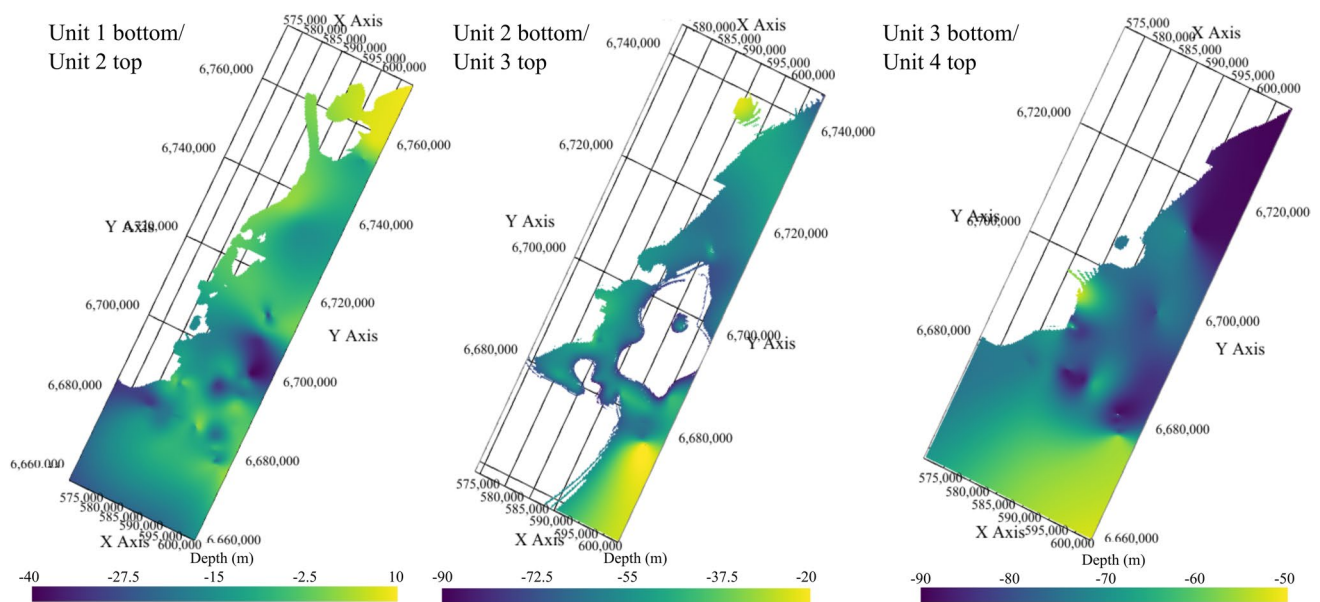


Fig. 11 Depth maps of GemPy-generated interface surfaces of the Pelotas Basin in the AOI. Each map shows the surface boundary between two units (base of upper unit and top of bottom unit, depth

relative to sea level). Empty areas show regions where the units were modeled as absent. Unit 1 bottom/Unit 2 top map does not consider surface topography. Note that scales are different for each map

The whole Pelotas Basin in the AOI (Model 3)

The 3D model generated by GemPy for the entire Pelotas Basin in the AOI is presented in Fig. 12, while Fig. 13 shows three 2D sections crossing the AOI. As mentioned

previously, Unit 4, composed mainly of argillaceous sediments of marine origin, represents the biggest volume of the basin, with thicknesses up to 470 m and maximum depth of 530 m. Discriminating this unit into sub-units was not possible with existing data and using the methods presented in

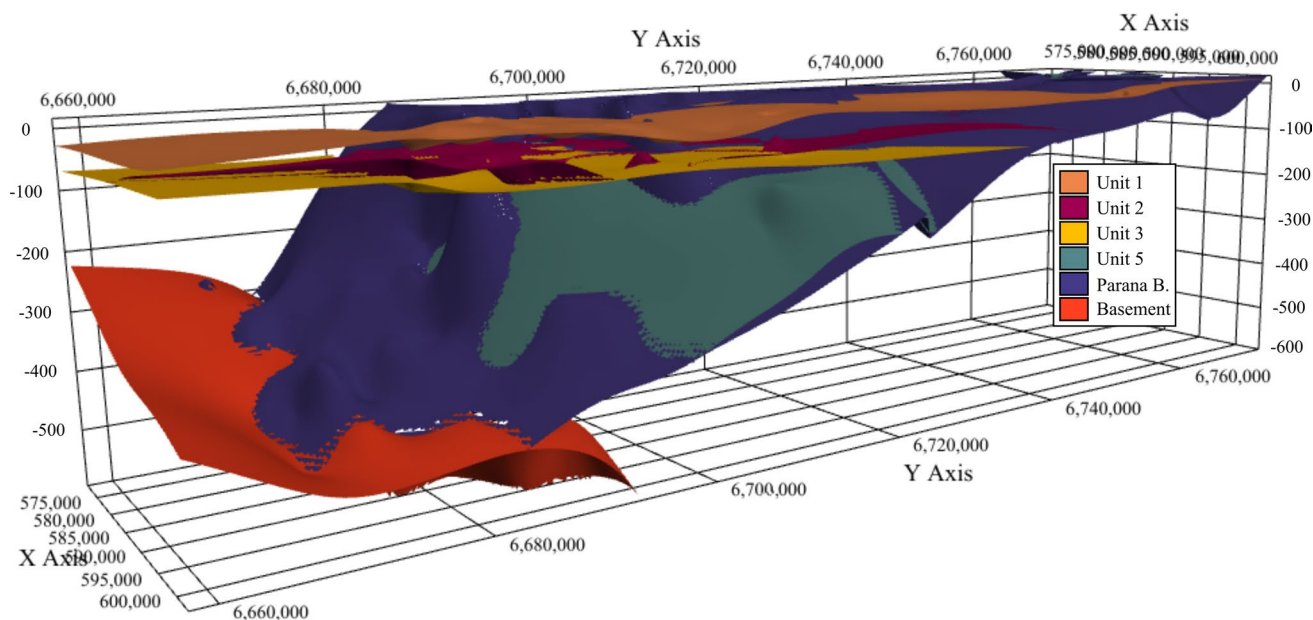


Fig. 12 Top 600 m of the model created, showing the Pelotas Basin and its units. Note that Unit 4 is not shown in the legend as it corresponds to all volume between Unit 3 and Parana Basin/Basement. The fifth unit will be detailed in “A Fifth Unit”. Vertical exaggeration: 200x

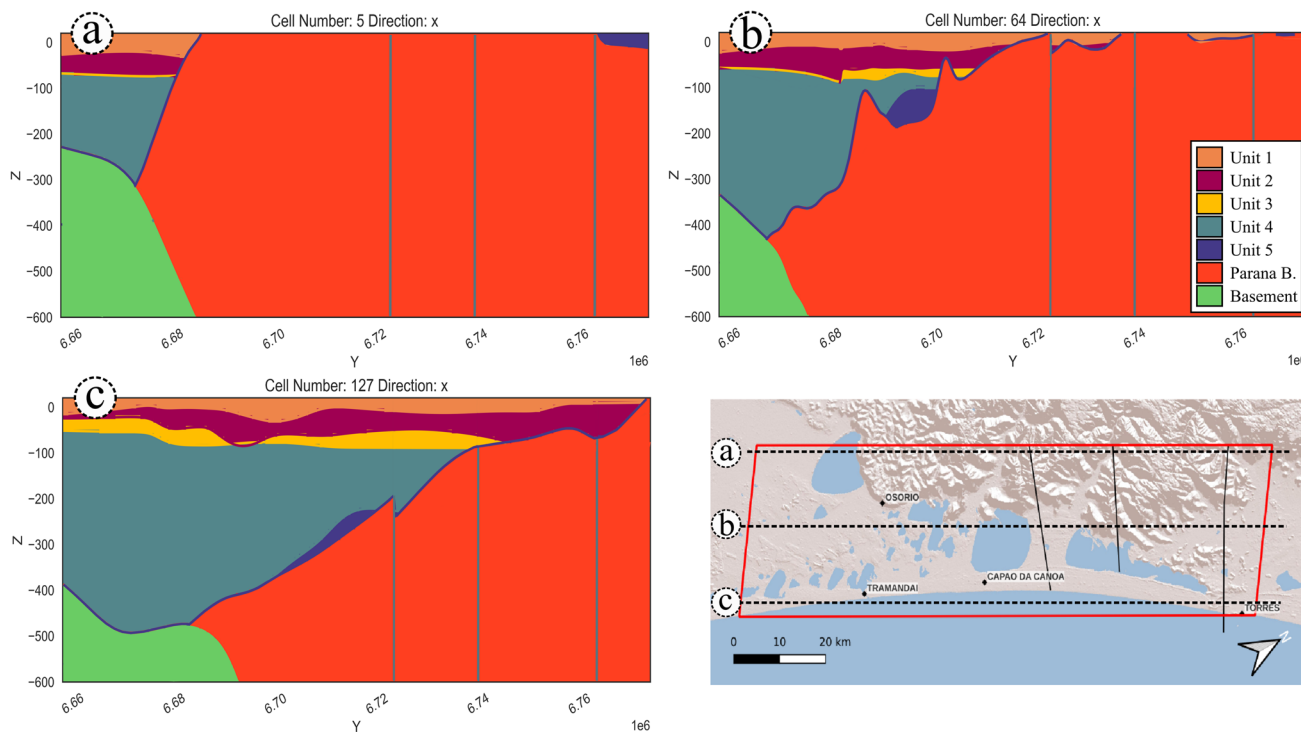


Fig. 13 Cross-sections of the modeled Pelotas Basin in the AOI for 600 m depth. The suggested fifth unit can be seen in cross-section “Geological and hydrogeological context” and “Materials and methods” as the purple area between Unit 4 and Paraná Basin. Vertical exaggeration: 100x

this work, mainly because of the great depths this unit starts to appear. Maximum depth of water wells drilled in the AOI is ~ 150 m, and thus the more detailed logs in this scale (SIA-GAS database) get only to the top of this unit. The deeper exploratory wells from the CEP database aimed at reaching older rocks, and did not focus on logging the Cenozoic: some drillings logged only parts of the Cenozoic sediments; other logs are not detailed enough only recording significant changes such as sand to clay or clay to alluvial deposits; some are even missing the Cenozoic sediments entirely.

Nonetheless, existing data allowed the separation of ‘Unit 4’ from what is suggested here would be a fifth unit, due its differing lithologies comparing to Unit 4. Although this fifth unit was only identified in five logs (3 CEP, 2 SIAGAS), the authors understand the geometry generated is a coarse-resolution representation of the real, in-depth layer. Due to the way GemPy works (modeling the bottom of a unit), in the model presented here this unit appears as part of the ‘Pelotas Basin Lower’ unit, and corresponds to the volumes seen in the model as ‘Pelotas Basin Lower’ (in opposition to the surface of ‘Pelotas Basin Lower’ running across the whole AOI marking the bottom of the basin). This unit will be detailed in “[A fifth unit](#)”, but can be briefly seen in Figs. 12 and 13.

Discussion

A fifth unit

As mentioned in “[The whole Pelotas Basin in the AOI \(Model 3\)](#)”, a lithology that can be separated from Unit 4 due to its contrasting lithology was identified in 5 geological logs (3 CEP, 2 SIAGAS). While Unit 4 is genetically linked to a marine environment and is observed in the logs as mainly clay deposits intercalated with other fines, this fifth unit presents coarser sediments. It appears in the logs mostly identified as ‘conglomerate rock’ (4 logs), but also as ‘medium to coarse sand’ with intercalations of fine sand and clay (1 log), below Unit 4 in the drilling logs. The ‘conglomerate rock’ entries in the logs might correspond, in fact, to deposits of mixed gravel, sand and finer sediments expected for the alluvial fans first described by Villwock (1984) and later detailed by Tomazelli and Villwock (2000). Thus, the existence of this unit is not unexpected, but to our knowledge it hasn’t been identified and modeled in previous works.

There is limited data other than the geological logs to support this possible unit, though. Two of the three geological logs from the CEP database where those coarser sediments were identified, GT-05 and GT-07, had geophysical profiles: natural gamma and spontaneous potential, respectively. While in the natural gamma profile from GT-05 there are no changes at the depth this possible unit appears (333 to 344,5 m), in the GT-07 spontaneous potential profile it is

visible a slight change of pattern, increasing values at the top of the lithology (147 m) and decreasing at the bottom (178 m). Unfortunately, there is no isotopic and/or hydrochemical data for the SIAGAS wells whose logs were interpreted as reaching this fifth unit. While well 4,300,008,746 located in Capão da Canoa is screened in multiple sedimentary layers, well 4,300,024,097 located in Osório was not screened in this alluvial fan sediments.

It is necessary to investigate this potential unit further to confirm its existence, and if so, to define its chemical and hydraulic characteristics, as well as to constrain the unit’s geometry.

Nonetheless, its identification in this work is seen as an advance in the geologic understanding of the AOI. An interesting point to observe and further investigate is the recharge mechanism of this unit. While Unit 4 might act as a hydraulic barrier, restricting or even impeding groundwater flow to this fifth unit, we hypothesize its recharge might occur in different ways: (1) from a possible connection with the other units due to this unit’s geometry, a high angled layer in the shoulders of the Paraná Basin, while the others are horizontal/semi-horizontal layers. The model computed in this work suggests this possibility is plausible (Fig. 14); (2) from the Paraná Basin itself in areas where the regional lineaments are present near the fifth unit, because they might generate a preferred pathway for groundwater recharge. This is also plausible, as the geometry of this unit, as computed in this work, extends to an area near one regional lineament. Nonetheless, those two hypotheses should be taken skeptically, considering the scarce evidence available to compute the geometry of this unit.

Comparing unit 3 extension with previous works

Unit 3 is also known as the ‘Coarse Salt’ (*Sal Grosso*) aquifer in the Northern Coast of Rio Grande do Sul, and was detailed in the works of Troian et al. (2020) and Collischonn and da Camara Rosa (2022); the latter identified the unit in several VES and SIAGAS well logs of Tramandaí and Osório (cities within this work’s AOI), and interpolated their results to create an extent map of the aquifer top (interface with Unit 2 bottom). In this section, results from this work are compared with the extent map of Unit 3 top from Collischonn and da Camara Rosa (2022). Focus is given to the southern half of the AOI, both because the work of Collischonn and da Camara Rosa (2022) is for this region (‘Previous work AOI’ in Fig. 15) and because to the north of Capão da Canoa city, there are only scarce points that do not add detail to the geometry of this unit, only indicating continuity (“[The top 150 m \(Model 2\)](#)”) presents the depth maps of Unit 3 top and base for the whole AOI). It is of note, though, that there are limitations to this comparison considering that this work encompasses a larger area, more data, and that, as

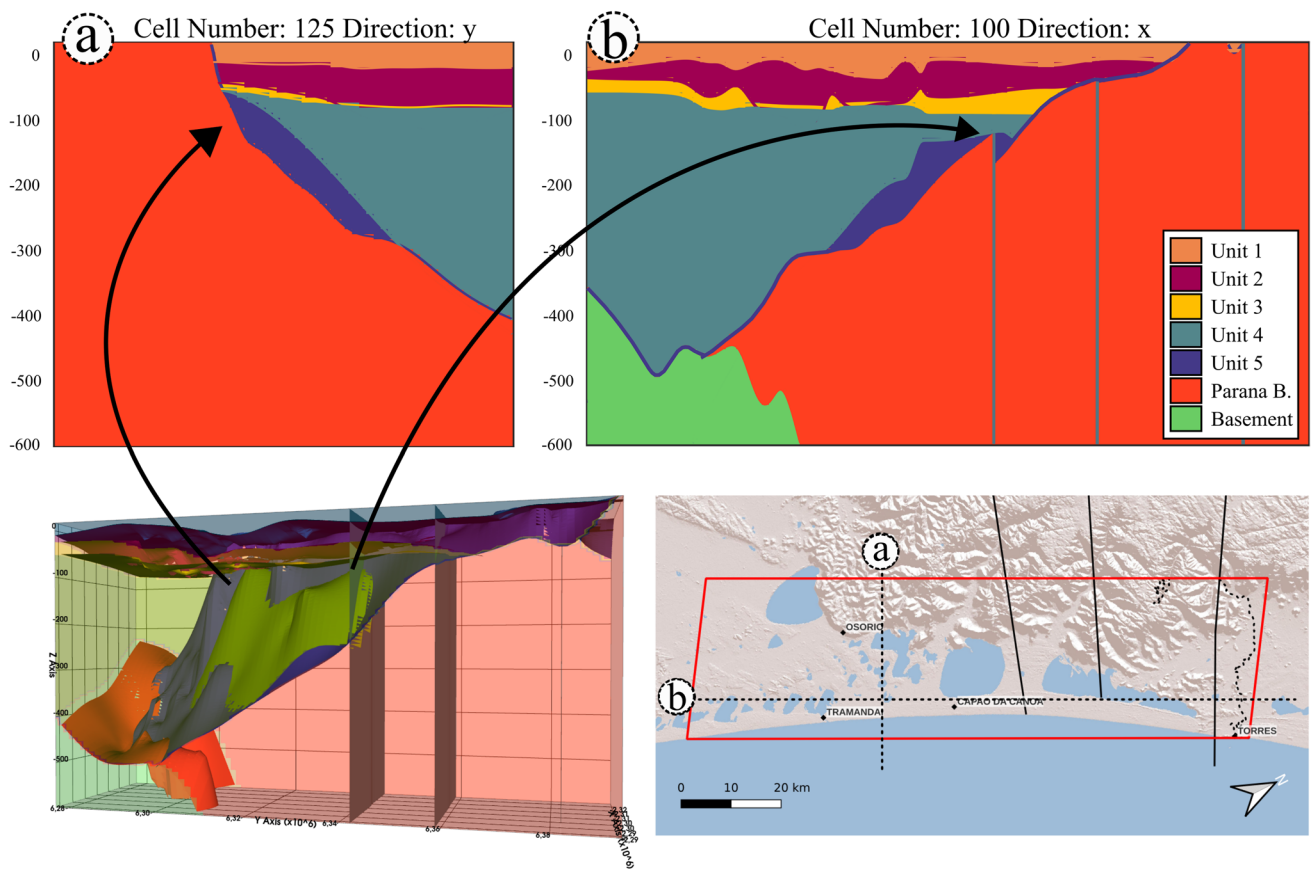


Fig. 14 Possible ways of groundwater recharge of the alluvial fans (here called fifth unit) identified in the AOI, illustrated by two 2D cross sections and the 3D model down to 600 m: (1) from possible connections with other sedimentary units due to the geometry of

this unit; (2) from the Paraná Basin itself in areas where the regional lineaments are present near the fifth unit. Note that the regional lineaments do not cross the Pelotas Basin sediments, only the area's basement (Paraná Basin and Precambrian rocks)

mentioned in “[Three-dimensional modeling](#)” and detailed in “[Model limitations](#)”, the input of VES data in this model was carried out using a different approach than the work by Collischonn and da Camara Rosa (2022).

A comparison between the extent of the top of Unit 3 according to this work and to Collischonn and da Camara Rosa (2022). As would be expected, considering that our work used data from theirs, the extents present similarities, but differences can also be seen in areas where the two works overlap. It is possible to observe that the model was able to closely replicate the limits of Unit 3 near Osório city, near the Paraná Basin outcrop and to the south of the city, and it is still possible to see the elongated feature in an NW–SE direction and perpendicular to the current coastline that the previous work modeled. But as one moves further from Osório, differences start to increase. A significant difference shows midway from Osório and Tramandaí, where the previous work estimated Unit 3 to be a wider feature in the NW–SE than this work, 1.4–5 km broader in some places. This work estimation also differed from the previous

work in modeling a small, isolated area of Unit 3 to the north of Tramandaí, while the previous work modeled it as a contiguous area. Other issues to consider when looking at this comparison are: there is no direct evidence that Unit 3 extends further south than shown in Fig. 15, although there are input points for other units, meaning GemPy might have considered those in the computation and extended the unit to the southernmost limit of the area. Similarly, there is no direct evidence (no data points) that the unit extends into the sea as modeled, although the aquifer was deposited during a lowstand system tract (Collischonn and da Camara Rosa 2022). Until further works are carried out to better constrain this unit, those extensions are considered as artefacts of the model.

Model limitations

The hydrostratigraphical model presented in this work is considered by the authors to be an important advance in the knowledge of the AOI, but we acknowledge there

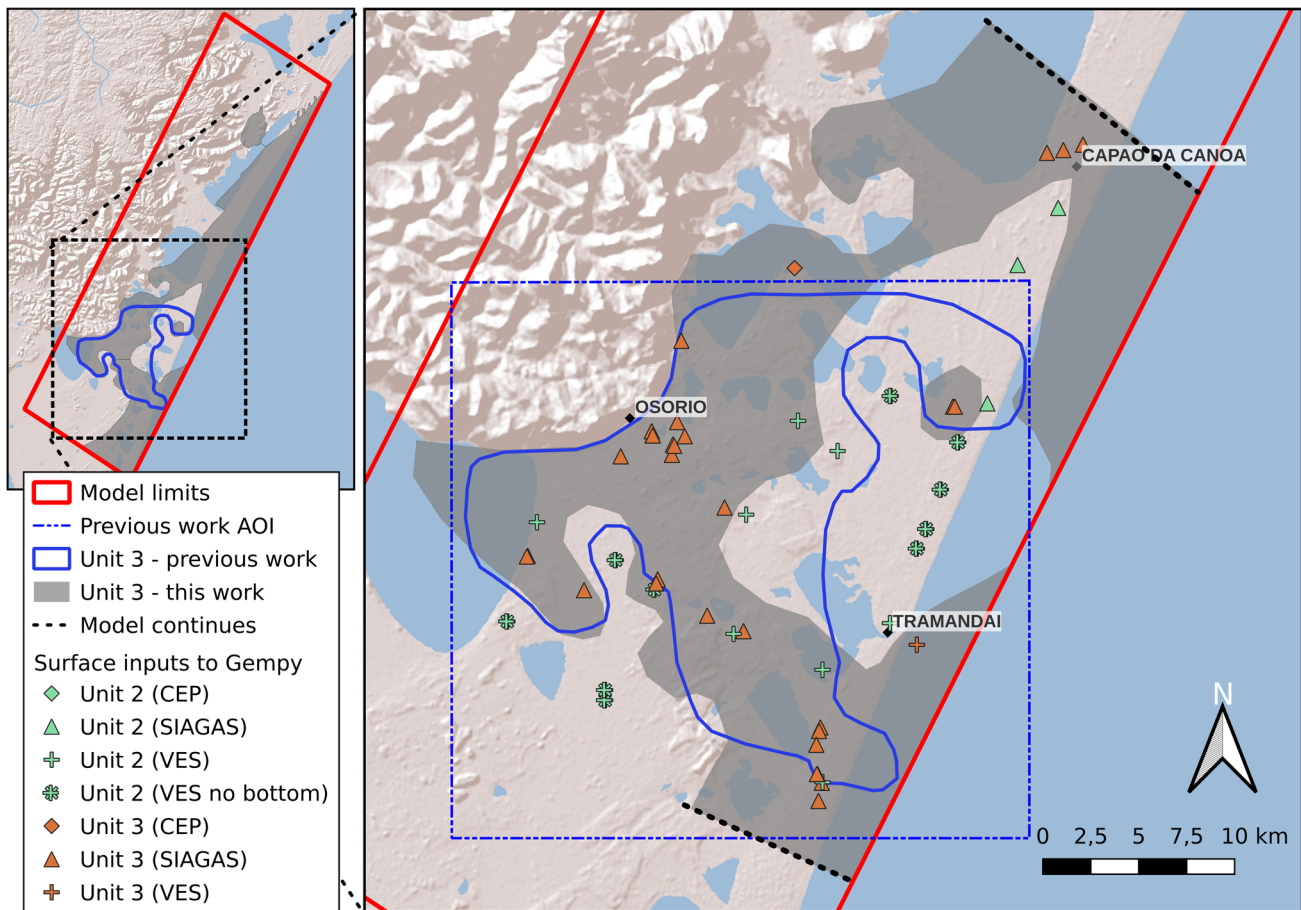


Fig. 15 Top of Unit 3 extent (‘Coarse Salt’ aquifer) as in this work and in Collischonn and da Camara Rosa (2022) (‘Previous work’ and ‘Previous work AOI’). Points indicate where Unit 2 and Unit 3 were identified in drilling logs or VES and used as input for this work (considering the bottom of units). Label “Unit 2 (VES no bottom)” indicates VES points from Collischonn and da Camara Rosa (2022)

that the bottom of unit 2 was not reached but the model was underestimating layer thicknesses if those points were not added (VES 2, 3, 6, 8, 10, 11, 16, 17, 18 and 19 – see “Three-dimensional modeling”). Black, dashed line in the main image indicates the unit extents south and north in the model; to the north, there are few points where Unit 3 was identified, and to the south, there are no input points

are several limitations to the current version of it. Further works need to be developed considering those limitations:

- **Model extent and coordinates:** GemPy currently works only with model extents that are a north–south and east–west aligned rectangle; also there is no way to mask off undesired areas. The regular solution to this issue would be to model a wider area, a north–south oriented rectangle that would encompass the ‘tilted’ AOI rectangle shown in the figures of this work. Another, more complex solution was chosen, that involved applying a 2D matrix rotation to our desired AOI extent and input points using GemGIS. This significantly reduced the extent of the model from an area of ~9500 km² in the regular approach to ~3600 km², and allowed a higher resolution model of the AOI instead of using resources to model undesired areas

- around it. The drawback of this approach, though, is that the rotation distorts the coordinates of the input points and output surfaces. When the model is rotated back to its original position (also using GemGIS), the coordinates are not correct and eventual exported meshes (e.g. VTK files) need to be georeferenced.
- **Rough Paraná Basin limits:** Another issue related to computing power is the definition of the Paraná Basin outcrop with a rough boundary (‘Paraná Basin Outcrop’ points in Fig. 3a). Initially this boundary was set with 150 input points delineating the basin in a higher resolution, to consider for local variations and alluvial deposits outside of the coastal area (rivers draining from the higher lands). As the model was not computing (crashing), this number was reduced to 87, then again to 40 points, which was an adequate number that allowed the

model to run with stability and still represents the outcrop of this basin.

- **Unit 2 thickness underestimation:** The usual method of inputting data to GemPy is considering the base of an unit. Nonetheless, for 11 of the 19 VES profiles from Collischonn and da Camara Rosa (2022) this work used a different approach. Those VES profiles identified Unit 1 and Unit 2, and observed Unit 2 to be a thick layer, not being able to reach the bottom of it to a depth of 110 m (method/set-up maximum depth). Our first approach was to leave those 11 VES profiles out of the GemPy input files, but this caused the model to underestimate Unit 2 layer thickness in the region, sometimes by more than 50% of thickness found in the VES profiles. Thus, in those profiles the VES depth (~ 100–110 m) was considered as the bottom of the unit. While this approach also underestimates Unit 2 real thickness, it presents lower uncertainty than our first approach. A probabilistic modeling and Bayesian Interference might be a way forward to improve this layer's estimation, that can be developed in future works due to the complexity involved.
- **Data reliability:** The Northern Coast of Rio Grande do Sul presents a relatively high number of borehole logs, but the geological value of individual borehole records is dependent on the skill and training of the supervisors responsible for logging the drilling process. If the supervisor is not well trained, equipped and supported then the information obtained is of little value for a groundwater study. A second point is that different companies might have different log approaches, meaning that the same borehole can be described in varied ways by different teams. While Troian et al., (2020) used 15 geophysical logs (natural gamma, electric resistivity and sonic profiles) and several water quality analysis (TDS) along 107 borehole logs to develop the hydrostratigraphical conceptual model of the Northern Coast of Rio Grande do Sul, and Collischonn and da Camara Rosa (2022) carried out 19 VES along the analysis of 29 borehole logs, the authors of this work understand borehole logs are still the main source of information for the AOI. Thus, there is a need for the expansion of works involving down-the-hole geophysics, VES, and other indirect methods in the AOI, as they are less prone to the uncertainties mentioned previously in this paragraph. Also, those methods would be extremely useful considering the highly dynamic systems that deposited the sediments in the AOI and generated, along with vertical variations, also horizontal changes that might not be fully understood only with 1D data (borehole logs).
- **Data limitation:** As one can see in the distribution of input points for the model (Fig. 3), there is limited data in the central and north parts of the AOI. The data was enough to allow for modeling of the units, but to refine

the model, more data in those regions would be needed. Also, we mentioned a fifth unit in the AOI hydrostratigraphy, but acknowledge this unit is observed only in a few points of data, and thus more studies focused on this unit would be necessary to characterize its geometry, extension, hydraulic properties and chemical composition of its waters.

Model findings and implications to groundwater management

Even with all limitations of the model and the need to refine it as mentioned in the previous section, it is still possible to use the current version to draw some conclusions regarding groundwater vulnerability and management. In this section, we evaluate the information available in the SIAGAS dataset in the light of Model 2, that focuses on the top 150 m of the basin. The SIAGAS dataset allows for drilling companies and users in general to input a variety of information regarding their wells, as for example well type, water use, geologic and constructive logs, hydrochemistry and pumping test data, and this information can then be downloaded by anyone. Nonetheless, some entries in the dataset are incomplete or inconsistent for the AOI, missing several fields, being possibly duplicates with different information, and sometimes only presenting well coordinates.

Still, by checking the modeled thicknesses of each unit in certain areas it is possible to estimate the degree of vulnerability to surface contamination of wells used for public supply within the AOI. From the 307 registered wells, there are 78 entries in SIAGAS identified as “public supply”, or drilled by municipalities or the state water and sanitation company (CORSAN) and thus assumed to be for public supply. From those, 29 wells are registered with “situation” as “pumping” or “equipped”—and thus active. This number seems rather low, as a recent national survey registered 51 public supply boreholes in the same area (ANA 2021). Unfortunately, the available data from this national survey is limited, and no geological or constructive information is available. Thus, the 29 entries from SIAGAS were used.

In Fig. 15, one can see the distribution of the 29 public supply wells. From this number, 55% (n = 16) did not present constructive information and screen position/length, while the remaining 45% (n = 13) had this information. Most of those 13 wells (n = 9) had screens in more than one depth, while the last 4 wells had single screens only. Wells screened in multiple depths might cause mix of waters from different layers or even hydrostratigraphical units, and thus cause contamination of the deeper ‘Sal Grosso’ aquifer (Unit 3). There are currently 5 public supply wells with multiple screens reaching this unit, and further investigations of those might help understand vulnerability of those to contamination.

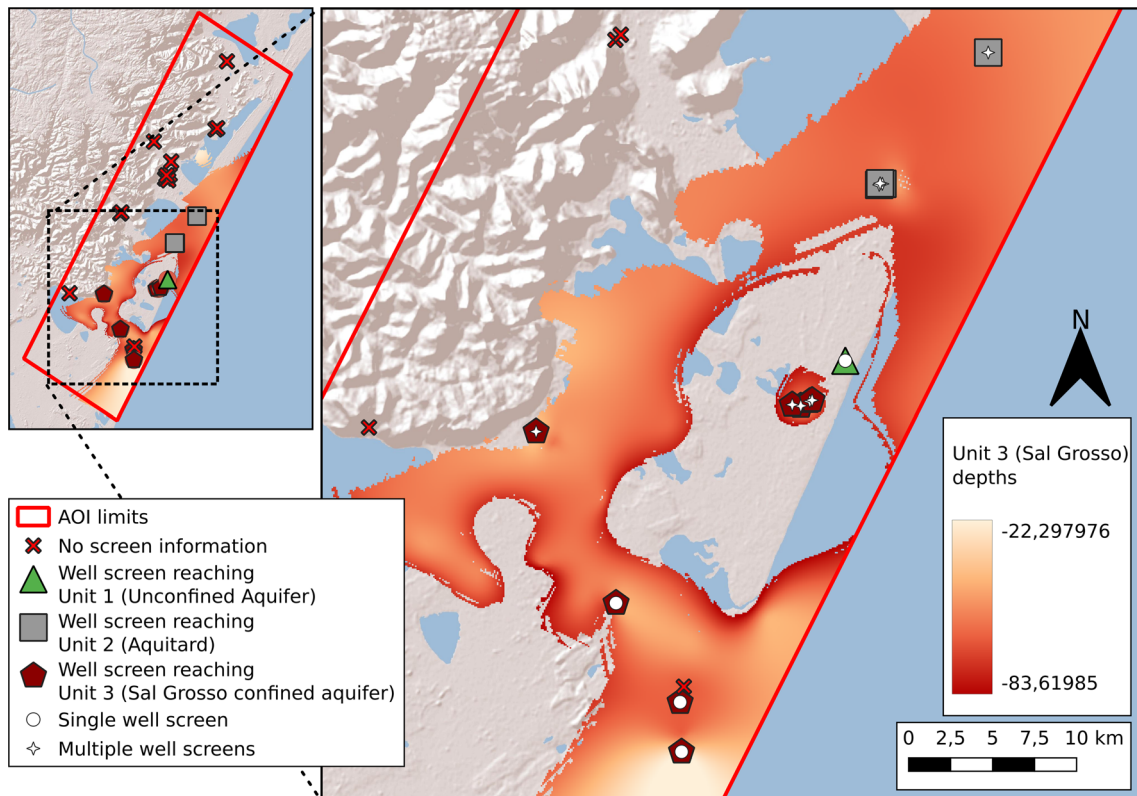


Fig. 16 Location of the 29 public supply wells in the AOI, with information of screen depth and type (single or multiple). Due to symbol size there are overlapping points in the figure

It is also possible to analyze the number of borehole drillings that reached or crossed Unit 3 (Sal Grosso aquifer), which could give an initial indication of the potential risk of contamination this unit is prone to. For this analysis, all boreholes with total drilling depth information were evaluated. We acknowledge that total drilling depth does not necessarily reflect to well depth, as the well could have been installed only to a certain depth of the bore. But consider that, ultimately, a drilling that reached Unit 3 using less-than-ideal practices of isolating geological layers and thus allowed hydraulic conductivity between Unit 1 (unconfined) and Unit 3 (confined) would be a potential source of contamination.

Based on this assumption, a total of 258 entries were retrieved from SIAGAS. Most of those, 204 wells or 79%, are outside the current delimitation of Unit 3 (Sal Grosso aquifer). For the ones inside the aquifer’s extension, 33 wells—13%—reach or cross the unit; other 17 wells—7%—reach Unit 2 (aquitarde) and the remaining 4 wells, or 1%, reach only Unit 1 (Fig. 16). From the 33 wells reaching or crossing Unit 3, 54% (n = 18) were drilled by CORSAN for public supply; wells drilled by

private companies account for 42% (n = 14) of entries, 4 of them being for monitoring purposes and managed by SGB-CPRM; The remaining 4%, or one well, was drilled by another state entity, the department of Works, Sanitation and Housing.

We further investigated those 33 entries to understand the current situation of those wells. Data was filtered for all entries related to “situation” as “abandoned”, “closed”, “stopped”, “not usable”, “not installed”, “obstructed” and “colmated” and “NULL” (not informed water use), as we understand those might pose the highest risks of contamination due to possible improper decommissioning. In total, 17 of those 33 wells, or 51% fall in one of those categories, although 9 of them were drilled by CORSAN and thus we understand were properly decommissioned. This leaves 8 wells, or 3% of the 258 wells, in a situation that might pose the highest risk of contamination of the Sal Grosso aquifer, as they were drilled by private companies that, although have technical expertise, might not have been requested by the borehole owners to decommission them (Fig. 17).

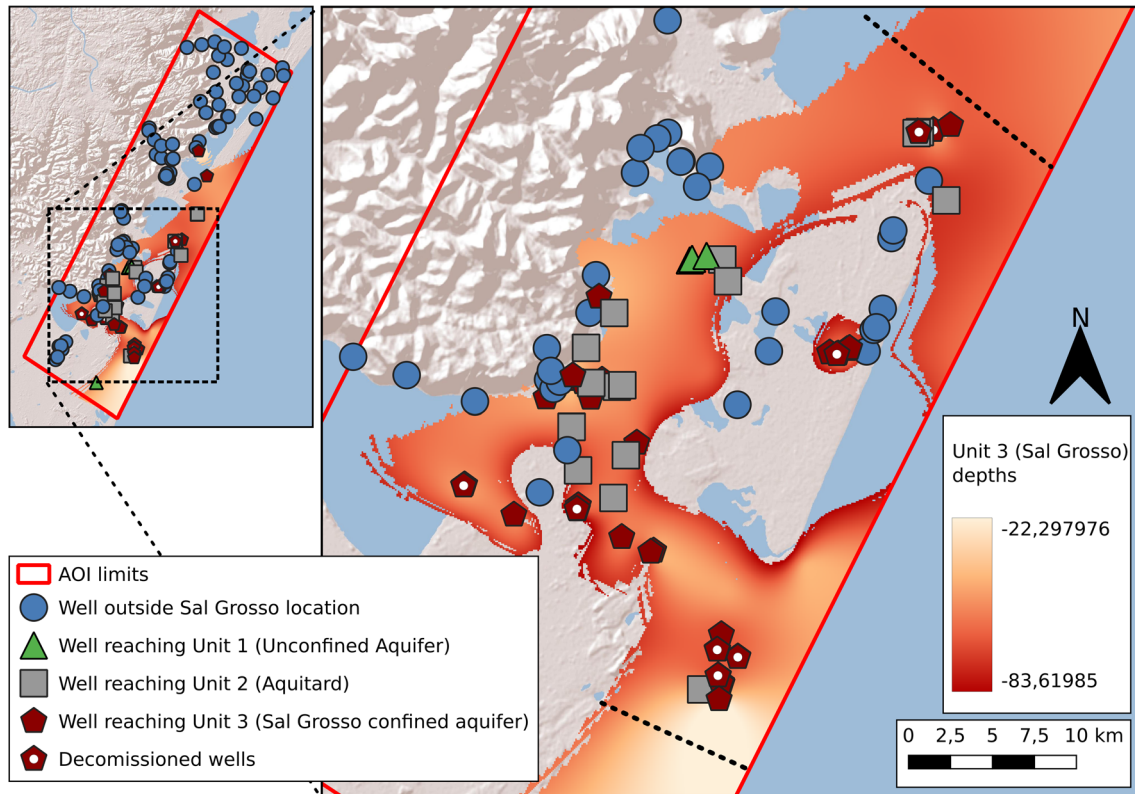


Fig. 17 Well situation comparing to Unit 3 extent and depth. Decommissioned wells were defined as the ones with the “situation” field as “abandoned”, “closed”, “stopped”, “not usable”, “not installed”,

“obstructed” and “colmated”, and are assumed to be more prone to contamination (see text). Due to symbol size there are overlapping points in the figure

Conclusions

In this work, a 3D hydrostratigraphical model of the Northern Coast of Rio Grande do Sul state was developed, aiming to improve the region’s geological and hydrogeological understanding, the communication of this comprehension to the general public, the groundwater management of the area aquifers and consequently to improve the resilience of the region against climate-change-expected sea level rise. Data from freely available data sources was used, as well as from previous works carried out in the AOI that characterized and detailed the hydrostratigraphical units of the area. This model was built using a free and open-source Python-based geomodeling library (GemPy) so its access can be free for the general public, academics, non-government organizations and other decision- and policy-makers.

This work consolidates and improves the understanding of the top four units existing in the area, showing them to be more heterogeneous in thickness and extent than previously thought. Unit 1 (aquifer) presents a thickness varying from 0 (absent, in the southern part of the AOI) to 40 m. Unit 2 (aquitard) was modeled as outcropping in the southern part of the AOI where

Unit 1 is absent, and presents a high variability in thickness—ranging from 10 to 90 m. Unit 3, an important aquifer in the region (‘Sal Grosso’ aquifer) presents a maximum thickness of 25–30 m in the southeast, but gets thinner to the northeast, being absent in the southwest and central parts of the AOI. Although the current model helped to better constrain Unit 3 geometry, its extension to the northeast is still uncertain and needs to be further investigated. Unit 4 showed to be the thicker unit in the region, up to 470 m thick and down to a maximum depth of 530 m. Subdividing this unit proved to be unviable with existing data, mostly focused in the top 150 m of the basin.

Along with the modeling of the four main hydrostratigraphical units, a fifth unit was observed in the data and modeled, that was associated with alluvial fans previously described in the literature but so far not identified in the region. Although, there is currently scarce evidence available to support the existence of this fifth unit, the authors hypothesize that, if this unit is indeed present in the area, its recharge mechanisms might be one or both of the following: (1) a connection with the other units due to this one’s geometry, a high angled layer in the shoulders of the Paraná Basin while the others are semi horizontal; (2) recharge through

the regional lineaments existing in the Paraná Basin that might be in contact with the fifth unit.

Based on the modeled surfaces, an investigation of the situation of public supply wells and of potential contamination of the ‘Sal Grosso’ confined aquifer was carried out. Results showed that, although there are 29 entries in SIAGAS for public supply, only 13 have information of screen depths. From those, 9 are multi screened wells, which could potentially cause mix of waters from different layers or even hydrostratigraphical units. In ‘Sal Grosso’, there are 5 multi-screened wells, and thus, further investigations on those wells to evaluate current and future vulnerability to contamination are recommended. It is also important to note that 29 entries might be an underestimated number, based on data from other sources.

Regarding potential contamination of the ‘Sal Grosso’ confined aquifer, from the 258 entries in SIAGAS for the AOI, it was observed that 54 wells are located in areas where the aquifer was modeled, and 33 of those (13%) reached or crossed the unit, most of them drilled by the state water and sanitation company. Considering the SIAGAS database, it is estimated that 3% of boreholes drilled in the AOI (8 wells out of the 258 entries) present a higher risk of contaminating the ‘Sal Grosso’ aquifer, as they have been drilled by private companies and are currently out of order—although it is unknown by the authors if those boreholes have been properly decommissioned.

To the present, it is understood that the ‘Sal Grosso’ aquifer is the most used aquifer for public supply in the AOI, although not widely utilized for other uses; the main reason possibly being the abundance of surface water and the easier accessibility to a shallower water supply, the unconfined aquifer in the AOI (Unit 1). This situation might change in the future with further population growth without proper expansion of sewage collection and treatment, that might reduce quality of water in the unconfined aquifer; climate change, sea level rise and intrusion of the saline wedge might also expand the use of ‘Sal Grosso’ aquifer, both due to reduced availability of surface water for irrigation and due to salinization of water from the top aquifer.

Further works are needed in the AOI to deepen the results of this work and close their gaps, as for example validate/characterize the alleged fifth unit, to refine current boundaries between the other four hydrostratigraphical units and to constrain Unit 3 (‘Sal Grosso’ aquifer) in detail. A robust geophysical logging survey might be useful to address the lack of data or inconsistencies observed in the geological logs. There is an abundance of drilled boreholes in the region, and logging strategic ones using electrical and nuclear probes that can be used in cased boreholes might fill existing gaps and uncertainties in this model. A complimentary method to be used in the

region could be surface Electrical Resistivity Tomography (ERT), that uses the same principle of resistivity as VES but create a two-dimensional cross sections of the electrical resistivity properties of the subsurface along a transect. Considering that Collischonn and da Camara Rosa (2022) applied VES investigations successfully to the AOI and that the hydrostratigraphical units in the area are heterogeneous, ERT surveys might help expand the knowledge in the area. We believe those further works would help to understand the hydrostratigraphy and the dynamic environment that generated the existing sedimentary layers in the Northern Coast of Rio Grande do Sul state, as well as feed the 3D geological model developed in this work.

Author contributions All authors contributed to the study conception and design. Data collection and initial analysis/processing was performed by L.M., who also drafted the first version of the manuscript and python code. Further versions of the manuscript were improved by L.M. and A.J. based on review and comments of all authors and reviewers. A.J. improved the python code. All authors read and approved the final manuscript.

Funding Open Access funding enabled and organized by Projekt DEAL. This work was supported by the Brazilian National Council for Scientific and Technological Development (*Conselho Nacional de Desenvolvimento Científico e Tecnológico – CNPq*) through a scholarship for L.M. in the National Institute of Science and Technology of the Cryosphere (*Instituto Nacional de Ciência e Tecnologia da Criosfera*). Open Access publication fees were covered by the German DEAL agreement.

Data availability and code All data and metadata used in this work can be found and downloaded in <https://github.com/lucianomarquetto/n-coast-RS>, along with the code developed for this model.

Declarations

Conflict of interest The authors have no relevant financial or non-financial interests to disclose.

Open Access This article is licensed under a Creative Commons Attribution 4.0 International License, which permits use, sharing, adaptation, distribution and reproduction in any medium or format, as long as you give appropriate credit to the original author(s) and the source, provide a link to the Creative Commons licence, and indicate if changes were made. The images or other third party material in this article are included in the article’s Creative Commons licence, unless indicated otherwise in a credit line to the material. If material is not included in the article’s Creative Commons licence and your intended use is not permitted by statutory regulation or exceeds the permitted use, you will need to obtain permission directly from the copyright holder. To view a copy of this licence, visit <http://creativecommons.org/licenses/by/4.0/>.

References

- Åberg SC, Åberg AK, Korkka-Niemi K (2021) Three-dimensional hydrostratigraphy and groundwater flow models in complex Quaternary deposits and weathered/fractured bedrock: evaluating

- increasing model complexity. *Hydrogeol J* 29(3):1043–1074. <https://doi.org/10.1007/s10040-020-02299-4>
- Agência Nacional do Petróleo - ANP (2023) Banco de Dados de Exploração e Produção. <https://www.gov.br/anp/pt-br>
- Agência Nacional de Águas e Saneamento Básico – ANA (2021) Atlas águas: segurança hídrica do abastecimento urbano. – Brasília. 332 p. Available at <http://atlas.ana.gov.br/>
- Bocanegra E, da Silva GC, Custodio E, Manzano M, Montenegro S (2010) State of knowledge of coastal aquifer management in South America. *Hydrogeol J* 18(1):261–267. <https://doi.org/10.1007/s10040-009-0520-5>
- Brasil. Ministério do Desenvolvimento Regional. Sistema Nacional de Informação sobre Saneamento (SNIS). 2023. Available at <http://app4.mdr.gov.br/serieHistorica/>
- Brisson S, Wellmann F, Chudalla N, von Harten J, von Hagke C (2023) Estimating uncertainties in 3-D models of complex fold-and-thrust belts: a case study of the Eastern Alps triangle zone. *Appl Comput Geosci* 18(October 2022):100115. <https://doi.org/10.1016/j.acags.2023.100115>
- Campbell D, de Beer J, Mielby S, van Campenhout I, van der Meulen M, Eriksson I, Ganerod G, Lawrence D, Bacic M, Donald A, Gogu CR, Jelenek J (2017) Transforming the relationships between geoscientists and urban decision-makers: European Cost Sub-Urban Action (TU1206). *Procedia Eng* 209:4–11. <https://doi.org/10.1016/j.proeng.2017.11.124>
- Chiles J-P & Delfiner P (2009) Geostatistics: modeling spatial uncertainty. J. W. & Sons (ed.); vol. 497
- Collischonn L, da Camara Rosa MLC (2022) Genesis of a coastal aquifer in the coastal plain of the Pelotas Basin, southern Brazil: implications for stratigraphic evolution. *J South Am Earth Sci* 116(December 2021):103801. <https://doi.org/10.1016/j.jsames.2022.103801>
- CPRM., Serviço Geológico do Brasil (2023) SIAGAS: Sistema de Informações de Águas Subterrâneas. Pumping well data in Brazil. <https://siagasweb.sgb.gov.br/layout/>
- Da Silva AF, Toldo EE, Van Rooijen A, De Abreu CF, Filho JLR, dos Da Rocha RS, Dos Santos Aquino R (2020) Coastal flooding by elevation of the sea level in Imbé and Tramandaí - RS. *Rev Bras Cartogr* 72(3):541–557. <https://doi.org/10.14393/rbcv72n3-48706>
- De La Varga M, Wellmann JF (2016) Structural geologic modeling as an inference problem: a Bayesian perspective. *Interpretation* 4(3):SM15–SM30. <https://doi.org/10.1190/INT-2015-0188.1>
- De La Varga M, Schaaf A, Wellmann F (2019) GemPy 1.0: open-source stochastic geological modeling and inversion. *Geosci Model Development* 12(1):1–32. <https://doi.org/10.5194/gmd-12-1-2019>
- Dillenburg SR, Tomazelli LJ, Martins LR, Barboza EG (2005) Modificações de Longo Período da Linha de Costa das Barreiras Costeiras do Rio Grande do Sul. *Gravel* 3(3):9–14
- Diniz JAO, Monteiro AB, Silva RC & Paula TLF (2014) Manual De Cartografia Hidrogeológica. Companhia de Pesquisa em Recursos Minerais (CPRM)
- Dramsch JS (2020) 70 years of machine learning in geoscience in review. *Adv Geophys* 61:1–55. <https://doi.org/10.1016/bs.agph.2020.08.002>
- Enemark T, Peeters LJM, Mallants D, Batelaan O (2019) Hydrogeological conceptual model building and testing: a review. *J Hydrol* 569:310–329. <https://doi.org/10.1016/j.jhydrol.2018.12.007>
- Famiglietti JS (2014) The global groundwater crisis. *Nat Clim Chang* 4(11):945–948. <https://doi.org/10.1038/nclimate2425>
- Foster S, Chilton J (2021) Policy experience with groundwater protection from diffuse pollution—a review. *Curr Opin Environ Sci Health* 23:100288. <https://doi.org/10.1016/j.coesh.2021.100288>
- Güdük N, De La Varga M, Kaukolinna J, Wellmann F (2021) Model-based probabilistic inversion using magnetic data: a case study on the kevitsa deposit. *Geosciences (switzerland)* 11(4):1–19. <https://doi.org/10.3390/geosciences11040150>
- Habel S, Fletcher CH, Rotzoll K, El-Kadi AI, Oki DS (2019) Comparison of a simple hydrostatic and a data-intensive 3d numerical modeling method of simulating sea-level rise induced groundwater inundation for Honolulu, Hawai’I, USA. *Environ Res Commun*. <https://doi.org/10.1088/2515-7620/ab21fe>
- Hirata R, Conicelli BP (2012) Groundwater resources in Brazil: a review of possible impacts caused by climate change. *An Acad Bras Ciênc* 84:297–312. <https://doi.org/10.1590/S0001-37652012005000037>
- Instituto Brasileiro De Geografia e Estatística - IBGE (2022). Censo Brasileiro de 2022. Rio de Janeiro: IBGE. <https://www.ibge.gov.br/estatisticas/downloads-estatisticas.html>
- Jüstel A, Correia AE, Pischke M, de la Varga M, Wellmann F (2022) GemGIS—spatial data processing for geomodeling. *J Open Source Software* 7(73):3709. <https://doi.org/10.21105/joss.03709>
- Kinkade D, Shepherd A (2022) Geoscience data publication: practices and perspectives on enabling the FAIR guiding principles. *Geosci Data J* 9(1):177–186. <https://doi.org/10.1002/gdj3.120>
- Kopp RE, Horton RM, Little CM, Mitrovica JX, Oppenheimer M, Rasmussen DJ, Strauss BH, Tebaldi C (2014) Probabilistic 21st and 22nd century sea-level projections at a global network of tide-gauge sites. *Earth’s Future* 2(8):383–406. <https://doi.org/10.1002/2014ef000239>
- Kumar CP (2013) Numerical Modelling of Ground Water Flow using MODFLOW. *Indian J Sci* 2(4):86–92. http://www.angelfire.com/nh/cpkbanner/publication/Modflow_Discovery.pdf
- Lajaunie C, Courrioux G, Manuel L (1997) Foliation fields and 3D cartography in geology: principles of a method based on potential interpolation. *Math Geol* 29:571–584
- Machado JLF & Freitas MAD (2005) Mapa Hidrogeológico do Rio Grande do Sul. Companhia de Pesquisa em Recursos Minerais (CPRM)
- Machado JLF, Faccini UF (2004) Influência Dos Falhamentos Regionais Na Estruturação Do Sistema Aquífero Guarani No Estado. XIII Congresso Brasileiro De Águas Subterrâneas 51:1–14
- Mader D, Schenk B (2017) Using free/libre and open source software in the geological sciences. *Aust J Earth Sci* 110(1):142–161. <https://doi.org/10.17738/ajes.2017.0010>
- Mahlknecht J, Mora A (2022) Editorial overview: management of groundwater resources and pollution prevention. *Curr Opin Environ Sci Health* 28:100365. <https://doi.org/10.1016/j.coesh.2022.100365>
- Mergel I (2015) Open collaboration in the public sector: the case of social coding on GitHub. *Gov Inf Q* 32(4):464–472. <https://doi.org/10.1016/j.giq.2015.09.004>
- Neumann B, Vafeidis AT, Zimmermann J, Nicholls RJ (2015) Future coastal population growth and exposure to sea-level rise and coastal flooding—a global assessment. *PLoS ONE*. <https://doi.org/10.1371/journal.pone.0118571>
- Philipp RP, Rolim SBA, Malta L, Jelinek AR, Viana A, Lavina E, Cagliari J & Faccini UF (2014) Estruturação do Arco de Rio Grande e da Sinclinal de Torres, Bacia do Paraná, RS - Evidências por Levantamentos Magnetotélúricos. Proceedings of the 6th Simpósio Brasileiro de Geofísica, January, 1–6. <https://doi.org/10.22564/6simbgf2014.026>
- Rosa MLCC, Tomazelli LJ, Costa AFU, Barboza EG (2009) Integração de métodos potenciais (gravimetria e magnetometria) na caracterização do embasamento da região sudoeste da bacia de pelotas, sul do brasil. *Revista Brasileira De Geofísica* 27(4):641–657
- Rosa MLCC, Barboza EG, Abreu VS, Tomazelli LJ, Dillenburg SR (2017) High-Frequency Sequences in the Quaternary of Pelotas Basin (coastal plain): a record of degradational stacking as a function of longer-term base-level fall. *Braz J Geol* 47(2):183–207. <https://doi.org/10.1590/2317-4889201720160138>

- Schaaf A, De La Varga M, Wellmann F, Bond CE (2021) Constraining stochastic 3-D structural geological models with topology information using approximate Bayesian computation in GemPy 2.1. *Geosci Model Development* 14(6):3899–3913. <https://doi.org/10.5194/gmd-14-3899-2021>
- Scott SW, Covell C, Júlíusson E, Valfells Á, Newson J, Hrafnkels-son B, Pálsson H, Guðjónsdóttir M (2019) A probabilistic geologic model of the Krafla geothermal system constrained by gravimetric data. *Geothermal Energy*. <https://doi.org/10.1186/s40517-019-0143-6>
- Terrington R, Napier B, Howard A, Ford J, Hatton W, Oleschko K, Cherkasov S, Prieto JLP, Argüelles VT, Salado CIG, Miranda AGC, Castro SAZ (2008) Why 3D? The need for solution based modeling in a national geoscience organization. *AIP Conf Proc* 1009:103–112. <https://doi.org/10.1063/1.2937278>
- Thomas AT, von Harten J, Jusri T, Reiche S, Wellmann F (2022) An integrated modeling scheme for characterizing 3D hydrogeological heterogeneity of the New Jersey shelf. *Mar Geophys Res* 43(2):1–19. <https://doi.org/10.1007/s11001-022-09475-z>
- Tomazelli LJ & Villwock JA (2000) O Cenozóico Costeiro do Rio Grande do Sul. In *Geologia do Rio Grande do Sul* (pp 375–406)
- Troian GC, Reginato PAR, Marquezan RG, Kirchheim R (2020) Hydrostratigraphy conceptual model of coastal aquifer system northern portion of the state of rio grande do sul. *Agua Subter-raneas* 34(3):264–274. <https://doi.org/10.14295/ras.v34i3.29883>
- Valeriano M, Rossetti D (2012) Topodata: Brazilian full coverage refinement of SRTM data. *Appl Geogr* 32(2):300–309. <https://doi.org/10.1016/j.apgeog.2011.05.004>
- Viero AC, Silva DRA, Zanini LFP, Hoelzel M, Dantas ME & Filho VO (2009) Mapa Geodiversidade do Estado do Rio Grande do Sul. Companhia de Pesquisa em Recursos Minerais (CPRM)
- Villwock JA (1984) Geology of the Coastal Province of Rio Grande do Sul, Southern Brazil. A synthesis. *Pesquisas Em Geociências* 16(16):5. <https://doi.org/10.22456/1807-9806.21711>
- Wellmann F, Caumon G (2018) 3-D Structural geological models: concepts, methods, and uncertainties. *Adv Geophys* 59:1–121. <https://doi.org/10.1016/bs.agph.2018.09.001>
- Wildner W, Ramgrab GE, da Lopes CR & da Iglesias CMF (2008) Mapa Geológico do Estado do Rio Grande do Sul 1: 750.000. Companhia de Pesquisa em Recursos Minerais (CPRM)
- Winner MD & Coble RW (1996) Hydrogeologic framework of the North Carolina Coastal Plain. *US Geological Survey Professional Paper*, 1404 I, 11–150
- Zuanazzi PT, Bartels M (2016) Estimativas para a população flutuante do Litoral Norte do RS. Porto Alegre: Fundação de Economia e Estatística

Publisher's Note Springer Nature remains neutral with regard to jurisdictional claims in published maps and institutional affiliations.